The growth of planetary embryos: orderly, runaway, or oligarchic?

R. R. Rafikov

Princeton University Observatory, Princeton, NJ 08544

ABSTRACT

We consider the growth of a protoplanetary embryo embedded in a planetesimal disk. We take into account the dynamical evolution of the disk caused by (1) planetesimal-planetesimal interactions, which increase random motions and smooth gradients in the disk, and (2) gravitational scattering of planetesimals by the embryo, which tends to heat up the disk locally and repels planetesimals away. The embryo's growth is self-consistently coupled to the planetesimal disk dynamics. We demonstrate that details of the evolution depend on only two dimensionless parameters incorporating all the physical characteristics of the problem: the ratio of the physical radius to the Hill radius of any solid body in the disk (which is usually a small number) and the number of planetesimals inside the annulus of the disk with width equal to the planetesimal Hill radius (which is usually large). We derive simple scaling laws describing embryo-disk evolution for different sets of these parameters. The results of exploration in the framework of our model of several situations typical for protosolar nebula can be summarized as follows: initially, the planetesimal disk dynamics is not affected by the presence of the embryo and the growth of the embryo's mass proceeds very rapidly in the runaway regime. Later on, when the embryo starts being dynamically important, its accretion slows down similar to the "oligarchic" growth picture. The scenario of orderly growth suggested by Safronov (1972) is never realized in our calculations; scenario of runaway growth suggested by Wetherill & Stewart (1989) is only realized for a limited range in mass. Slow character of the planetesimal accretion on the oligarchic stage of the embryo's accumulation leads to a considerable increase of the protoplanetary formation timescale compared to that following from a simple runaway accretion picture valid in the homogeneous planetesimal disks.

Subject headings: planets and satellites: general — solar system: formation — (stars:) planetary systems

1. Introduction.

It is now widely believed (e.g. Safronov 1991, Ruden 1999) that terrestrial planets (planets like Earth and Venus) have formed by agglomeration of numerous rocky or icy bodies called planetesimals (similar to the present-day asteroids, comets, and Kuiper Belt objects). Understanding this accretion process is central to understanding planet formation.

Since the pioneering work of Safronov (1972) it has been known that the dynamics of the planetesimal disk, namely the evolution of planetesimal eccentricities and inclinations, is a critical factor in this process because relative planetesimal velocities determine to a large extent the accretion rate of protoplanetary bodies. The dynamical state of the disk is affected by several processes. Gravitational scattering between planetesimals leads to the growth of their epicyclic energy, thereby increasing relative velocities in the disk. This interaction can proceed in two different regimes depending on the relation between the random velocity of planetesimals v relative to local circular motion and the differential shear across the Hill radius of two interacting bodies r_H:

$$r_H = a \left(\frac{m_1 + m_2}{M_c} \right)^{1/3}, \tag{1}$$

where m_1 and m_2 are the masses of the interacting planetesimals, M_c is the mass of the central star and a is the distance from the central star at which the interaction occurs. Scattering is said to be in the shear-dominated regime when $v \lesssim \Omega r_H$, and in the dispersion-dominated regime when $v \gtrsim \Omega r_H$ (Stewart & Ida 2000), where $\Omega = \sqrt{GM_c/a^3}$ is the rotation frequency of a Keplerian disk. Scattering in the first regime is strong for planetesimals separated by $\sim r_H$ and they can increase their random velocities very rapidly as a result of it. In the second regime scattering is mostly weak even at close encounters because relative velocities are large; in this regime it requires much more time to change the kinematic properties of planetesimals. Since scattering in the shear-dominated case is so efficient it is likely that this scattering would quickly heat up the disk and bring it into the dispersion-dominated regime. For example, a 50-km planetesimal (corresponding to a mass $\approx 10^{21}$ g) at 1 AU would enter the dispersion-dominated regime for interaction with other planetesimals when its epicyclic velocity is as small as 3 m s-1 (corresponding eccentricity is only 10^{-4}). Thus, it is plausible that at the evolutionary stage when the first massive bodies start appearing in the system, planetesimals interact with each other in the dispersion-dominated regime — an assumption which we will be using throughout this paper.

Later in the course of the nebular evolution, another dynamical excitation mechanism emerges: gravitational interaction with the newly born massive bodies. We call these bodies embryos (following Safronov 1972) since they are the precursors of the protoplanets; we will require that their masses be greater than the planetesimal masses. When these embryos become massive enough they excite planetesimal velocities in their vicinity and also change the spatial distribution of planetesimals around them. The importance of these effects was first emphasized by Ida & Makino (1993), who used N-body simulations to study planetesimal disks with embedded embryos.

Depending on the dynamical state of the planetesimal disk, protoplanetary growth can proceed in several different regimes. Safronov (1972) argued that emerging embryos heat the planetesimal disk up to the point where the random velocities of constituent planetesimals are of the order of the escape velocity from the most massive embryos. It is not clear, however, whether the embryo has enough time to increase planetesimal velocities to such large values given inefficiency of scattering in the dispersion-dominated regime. Stewart & Wetherill (1988) have noted the importance of the dynamical friction in the redistribution of random energy among planetesimals of different

masses and between planetesimals and embryos. They argued in favor of much smaller planetesimal epicyclic velocities which facilitates planetary accretion. However the spatially inhomogeneous character of the dynamical effects of the embryos on the disk were overlooked in their study.

To illustrate the difference between these two scenarios let us estimate the embryo's accretion rate dM_e/dt in the two-body approximation[1] (neglecting the gravity of the central star):

$$\frac{dM_e}{dt} \simeq \pi R_e^2 \Omega m N \frac{v}{v_z}\left(1+\frac{2GM_e}{R_e v^2}\right), \tag{2}$$

where m is the average planetesimal mass, M_e is the mass of the planet, R_e is its radius, N is the surface number density of planetesimals, and v_z is the average planetesimal velocity in the vertical direction (determining the disk thickness and, thus, the local volume density of planetesimals; it is usually of the same magnitude as v). The second term in brackets describes gravitational focussing, which can strongly increase the collision cross-section over its geometric value πR_e^2 when the planetesimal velocity is smaller than the escape speed from the embryo's surface $\sqrt{2GM_e/R_e}$. Safronov's (1972) assumption means that focussing is weak. Then one can easily show that

$$\frac{1}{M_e}\frac{dM_e}{dt} \propto M_e^{-1/3}, \tag{3}$$

i.e. the embryo's growth rate slows down as its mass increases. This type of planetary growth is known as *orderly* growth, because it implies that many embryos grow at roughly the same rate. On the contrary, if one neglects the embryo's effect on v and v_z and assumes focussing to be strong (following Wetherill & Stewart 1988) one finds that

$$\frac{1}{M_e}\frac{dM_e}{dt} \propto M_e^{1/3}, \tag{4}$$

i.e. embryo's growth accelerates as its mass increases. This corresponds to the so-called *runaway* accretion regime (Wetherill & Stewart 1989), which allows massive bodies grow very quickly[2] in contrast with the orderly growth picture. Note that the presence of the dynamical friction is not crucial for the onset of runaway growth (it only speeds it up) — what is important is the regulation of planetesimal velocities by planetesimal-planetesimal scattering, rather than embryo-planetesimal scattering which makes v and v_z independent of M_e.

However, it is also possible that effects of the embryo on the velocity dispersion are important but not so strong as orderly scenario assumes; in this case planetesimal velocities can be increased up to several ΩR_H, where $R_H = a(M_e/M_c)^{1/3}$ is the Hill radius of the embryo (note that it is considerably larger than the Hill radius r_H characterizing planetesimal-planetesimal scattering). Then formula (2) yields equation (3) but with a different proportionality constant. This regime is

[1]See also Kokubo & Ida (1996, 1998) for a similar discussion.

[2]Formally the condition (4) means that embryo reaches infinite mass in finite time given unlimited supply of material for accretion.

called *oligarchic* (Kokubo & Ida 1998) and is different from orderly growth because of the role of the gravitational focussing (it is very important in this regime) and the values of planetesimal velocities (they are much smaller than the embryo's escape speed). As a result, more massive embryos grow slower than the less massive ones (similar to orderly growth) but embryos still grow faster than planetesimals in their vicinity [similar to runaway growth, see Ida & Makino (1993)]. The accretion in the oligarchic regime is considerably slower than in the runaway regime but faster than in the orderly regime. For further convenience we briefly summarize major properties of all 3 accretion regimes:

- orderly — growth of velocity dispersion in the disk is dominated by the embryo, gravitational focussing is weak;
- runaway — velocity dispersion growth is determined solely by the planetesimal-planetesimal scattering, focussing is strong;
- oligarchic — velocity dispersion growth is dominated by the embryo, focussing is strong.

The growth timescale of the embryo is a very important quantity. The need for the giant planets to accrete their huge gaseous mass onto their rocky cores (core-instability model, see Mizuno 1980; Stevenson 1982; Bodenheimer & Pollack 1986) prior to the dissipation of the gaseous nebula (Hollenbach *et al.* 2000) constrains the growth timescale in the giant planet zone — between 5 and 30 AU in the protosolar nebula — to be $\lesssim 10^6 - 10^7$ yr. This interval must accommodate several distinct evolutionary stages — planetesimal formation from dust, planetesimal coagulation into protoplanetary embryos, and finally, catastrophic collisions between embryos to form rocky cores of giant planets. Thus, embryos have only part of this time available for their growth. Orderly growth is characterized by very long timescales — of order $10^8 - 10^9$ yr (Safronov 1972). On the contrary, runaway growth allows embryos to reach $\sim 10^{26}$ g (approximately the mass of the Moon) in about 10^5 yr (Wetherill & Stewart 1993). Runaway growth stops at approximately this mass because the embryo accretes all the solid material within its "feeding zone" — an annulus with the width of several R_H (Lissauer 1987). This mass is sometimes called the *isolation* mass M_{is} (see §3.1).

The dynamical effects of the embryo on the disk, as described numerically by Ida & Makino (1993) and Tanaka & Ida (1997) and analytically by Rafikov (2001, 2002a, 2002b, hereafter Papers I, II, & III correspondingly) and Ohtsuki & Tanaka (2002) are likely to change this conclusion. The results of these studies indicate that even if the mass of the embryo is much smaller than the isolation mass it will dominate the dynamical evolution of the nearby region of the disk, which brings the accretion into the much slower oligarchic mode. In this case the timescale required to achieve M_{is} becomes longer than that predicted by a simple picture of the runaway growth.

In this paper we study the coupled evolution of the planetesimal disk and protoplanetary embryo. Our goal is to determine (1) which conditions need to be fulfilled for the aforementioned regimes to be realized in protoplanetary nebula, (2) whether there are transitions between them

and when do they occur, (3) which regime sets the timescale for the planetary growth in the disk. To answer these questions we consider a very simple model of the embryo-planetesimal disk system. We describe the behavior of the disk by representing it as a planetesimal population with a single nonevolving mass m [similar to "monotrophic" model of coagulation of Malyshkin & Goodman (2001)]. This assumption might seem to be a gross oversimplification but even this toy model can still give us a lot of insight into the details of embryo-disk dynamics. The most important omission for the dynamics of the system which we make by employing this assumption is the absence of dynamical friction within the planetesimal disk. But, as we have mentioned above, this cannot preclude the runaway growth from happening. Also, when runaway or oligarchic regimes take place, the most massive body in the system grows faster than lower mass planetesimals because the growth rate increases with mass in these accretion regimes, see equations (2) and (4). This justifies our assumption of nonevolving planetesimal mass. We devote more time to the discussion of the accuracy of our approximations in §4.

The spatially resolved evolution of the kinematic properties of the disk and the growth of the embryo's mass are considered simultaneously and self-consistently within the framework of our model. This distinguishes our approach from both conventional coagulation simulations which neglect spatial nonuniformities of the disk properties caused by the embryo's presence (Wetherill & Stewart 1993; Kenyon & Luu 1998; Inaba *et al.* 2001) and purely dynamical estimates which do not allow the embryo's mass to vary[3] (Ida & Makino 1993; Paper I; Ohtsuki & Tanaka 2002). To describe the coupling between the disk dynamics and embryo's mass growth we use a set of equations describing both the planetesimal-planetesimal and the embryo-planetesimal gravitational interactions which were derived in Papers II & III correspondingly. Their validity has been checked elsewhere using direct integrations of planetesimal orbits in the vicinity of the embryo (Paper III). These analytical equations are solved numerically in §3. In addition, to highlight the importance and better understand the behavior of different physical processes operating in the system we provide simple scaling estimates for the evolution of the disk kinematic properties and the growth of the embryo's mass in §2. We discuss the applications and limitations of our analysis in §4.

We will often use the model of the Minimum Mass Solar Nebula (MMSN, Hayashi 1981) to obtain typical numerical values of physical quantities. In particular, we will use the following distribution of the surface mass density of the solids in MMSN (Hayashi 1981):

$$\Sigma = 20 \text{ g cm}^{-2} \left(\frac{a}{1 \text{ AU}}\right)^{-3/2}, \tag{5}$$

which is obtained assuming that solids constitute $\approx 1\%$ of the nebular mass.

[3]Probably the closest analog of our method is the multi-zone coagulation simulations of Spaute *et al.* (1991) and Weidenschilling *et al.* (1997).

2. Scaling arguments.

In this section we provide simple scaling-type solutions describing the coupled evolution of the embryo-planetesimal disk system. The reader interested only in the numerical results of more detailed and accurate calculations can skip this section and proceed directly to §3.

We first derive a set of evolution equations for the embryo's mass growth and for the planetesimal velocity dispersions in the horizontal and vertical directions using qualitative reasoning. This will allow us to better understand different dynamical mechanisms operating in the disk and predict the dependence of the system's behavior on its basic parameters. The equations are derived for two different regimes of the embryo-planetesimal gravitational interaction — dispersion-dominated and shear-dominated, although we mostly concentrate our attention on the former. We will assume that planetesimal-planetesimal interactions always occur in the dispersion-dominated regime which almost certainly should be true. From now on by different velocity regimes we will imply different regimes of the embryo-planetesimal interaction.

2.1. Derivation of the qualitative equations.

We start with the shear-dominated regime. In this case the approach velocity of a planetesimal towards the embryo is $\sim \Omega R_H$ and the effect of the tidal force of the central star is quite important. As a result scattering is strong and each encounter with the embryo imparts the planetesimal with a change of its velocity in the horizontal direction $\Delta v \sim \Omega R_H$ (Petit & Hénon 1986). At the same time the excitation of the vertical component of the planetesimal velocity is weak, because the thickness of the planetesimal disk is smaller than the embryo's Hill radius R_H. As a result, scattering is almost two-dimensional and scattered planetesimals are restricted to the plane of the disk. Only the deviations from purely planar geometry can lead to the growth of inclination. On the basis of geometric considerations we can predict that $\Delta v_z \sim (v_z/\Omega R_H)\Delta v \sim v_z$.

Planetesimals at different semimajor axes separations have different synodic periods (the time between successive conjunctions with the embryo). In the shear-dominated regime the most important region of the disk is that within a Hill sphere of the embryo. Planetesimals in this region have radial separations from the embryo $\sim R_H$ and travel past the embryo at relative velocity $\sim \Omega R_H$. Thus, the typical time between consecutive conjunctions with the embryo for planetesimals in this part of the disk is

$$T_{syn} = \frac{4\pi}{3}\Omega^{-1}\frac{a}{R_H} \sim \Omega^{-1}\frac{a}{R_H}. \tag{6}$$

Then we can approximately describe the dynamical evolution of the planetesimal disk due to the embryo in the shear-dominated regime as

$$\left.\frac{dv^2}{dt}\right|_{sd}^{em-pl} \approx \frac{\Delta v^2}{T_{syn}} \approx \Omega\frac{R_H}{a}(\Omega R_H)^2, \tag{7}$$

$$\left.\frac{dv_z^2}{dt}\right|_{sd}^{em-pl} \approx \frac{\Delta v_z^2}{T_{syn}} \approx \Omega \frac{R_H}{a} v_z^2. \tag{8}$$

We now turn to the dispersion-dominated regime, first focussing on embryo-planetesimal scattering. Here the two-body approximation usually proves to be very useful. In this approximation the influence of the third body — the central star — can be neglected and three-body scattering problem naturally reduces to the two-body problem which is tractable analytically. We will carry out our qualitative arguments using the instantaneous scattering approximation. In this approximation a body with a mass m_1 approaching another body with a mass m_2 with relative velocity v at an impact parameter b experiences a change in velocity roughly equal to $\Delta v \sim Gm_2/(bv)$ assuming small angle scattering. This approximation is valid if $b > b_0 \sim G(m_1 + m_2)/v^2$, since for $b < b_0$ large-angle scattering takes place. The upper bound on b is set by the smaller of the disk vertical thickness $H \approx v_z/\Omega \gg b_0$ and the range of planetesimal epicyclic excursions v/Ω (usually H is the one). Since in three-dimensional scattering every decade in the impact parameter b between b_0 and H provides roughly the same contribution to the scattering coefficients we find, integrating the expression for Δv over b, that the change of v^2 per encounter averaged over b is

$$\langle \Delta v^2 \rangle \approx \left(\frac{Gm_2}{v}\right)^2 \frac{\Omega^2}{vv_z} \ln \Lambda, \qquad \text{where} \quad \Lambda \approx H/b_0 \sim \frac{v_z v^2}{(\Omega a)^3} \frac{M_c}{m_1 + m_2}. \tag{9}$$

Changes of v^2 and v_z^2 are different only by constant factors because scattering has a three-dimensional character in the dispersion-dominated regime.

Embryo-planetesimal scattering leads to changes of planetesimal velocity only at conjunctions with the embryo. Planetesimals which can experience close encounters with it occupy an annulus of the disk with width $\approx v/\Omega$ around the embryo's orbit. The typical time between the consecutive approaches to the embryo for the planetesimals in this zone is $\sim T_{syn}(\Omega R_H/v)$. Then we can write the following equation for the velocity evolution caused by the embryo-planetesimal encounters in the dispersion-dominated regime:

$$\left.\frac{d}{dt}\left(v^2, v_z^2\right)\right|_{dd}^{em-pl} \approx \frac{\langle \Delta v^2 \rangle}{T_{syn}} \frac{v}{\Omega R_H} \approx \Omega \frac{R_H}{a} \frac{(\Omega R_H)^5}{v^2 v_z} \ln \Lambda_e, \tag{10}$$

where Λ_e is Λ computed using $m_2 = M_e \gg m = m_1$.

We next turn to planetesimal-planetesimal scattering, which always occurs in the dispersion-dominated regime (see §1). The volume number density of planetesimals n can be expressed through the surface number density N as $n \simeq N/H \approx N\Omega/v_z$. Then we can write the rate of random velocity growth in the disk due to planetesimal-planetesimal encounters as

$$\left.\frac{d}{dt}\left(v^2, v_z^2\right)\right|_{dd}^{pl-pl} \approx vn \frac{vv_z}{\Omega^2} \langle \Delta v^2 \rangle \approx \Omega N r_H^2 \frac{(\Omega r_H)^4}{vv_z} \ln \Lambda_p, \tag{11}$$

where m is the typical planetesimal mass and Λ_p is the value of Λ calculated using $m_1 = m_2 = m$. More accurate forms of the velocity growth equation (11) in the dispersion-dominated regime have been previously obtained by a number of authors (Stewart & Wetherill 1988; Ida 1990; Stewart & Ida 2000; Paper II). One can compare them with (10) and see that our equation really is a qualitative version of more accurate results.

The embryo's accretion rate can also be approximated by the two-body expression (2). We will assume that the physical collisions between the embryo and planetesimals occur with velocities at infinity considerably smaller than the embryo's escape velocity. This assumption, which implies that gravitational focussing plays an important role in the accretion process, is usually justified in the early stages of the embryo's growth but can run into problems later if planetesimal disk heats up very strongly. We will later check the validity of this assumption (see §4). In the shear-dominated regime the approach velocities of planetesimals are dominated by the differential shear in the disk, i.e. $v \sim \Omega R_H$. In the dispersion-dominated regime the approach velocities are dominated by the epicyclic motion of planetesimals. As a result we find that

$$\dot{M}\Big|_{sd} \approx mN\frac{(\Omega R_H)^2}{v_z}R_e \tag{12}$$

in the shear-dominated regime, and

$$\dot{M}\Big|_{dd} \approx mN\frac{(\Omega R_H)^3}{vv_z}R_e \tag{13}$$

in the dispersion-dominated regime. More accurate expressions for the accretion rate in these regimes can be found in Greenzweig & Lissauer (1992) and Dones & Tremaine (1993).

At this point it is useful to switch to the following dimensionless notation

$$\begin{aligned} &s^2 = \frac{\langle v^2\rangle}{(\Omega r_H)^2}, \quad s_z^2 = \frac{\langle v_z^2\rangle}{(\Omega r_H)^2}, \quad \mathcal{M} = \frac{M_e}{m}, \quad p = \frac{R_e}{R_H}, \\ &\tau = t/t_{syn}, \quad \text{where} \quad t_{syn} \equiv \frac{4\pi}{3}\Omega^{-1}\frac{a}{r_H} = T_{syn}\frac{R_H}{r_H} = T_{syn}\mathcal{M}^{1/3}, \end{aligned} \tag{14}$$

i.e. we normalize the planetesimal velocities by the shear across the planetesimal Hill radius $r_H = a(m/M_c)^{1/3}$, time by synodic period at 1 r_H and embryo's mass by the planetesimal mass m. The parameter p is the ratio of the embryo's physical radius to its Hill radius, which remains constant as the embryo grows at constant density. Note that in this notation embryo-planetesimal interaction is in the shear-dominated regime when $s \lesssim \mathcal{M}^{1/3}$, and in the dispersion-dominated regime when $s \gtrsim \mathcal{M}^{1/3}$.

With these definitions we can rewrite the equations governing the behavior of the planetesimal velocity and embryo's mass growth in the following dimensionless form: in the shear-dominated regime ($s \lesssim \mathcal{M}^{1/3}$)

$$\frac{ds^2}{d\tau} \approx (Nar_H)\frac{\ln\Lambda_p}{ss_z} + \mathcal{M}, \tag{15}$$

$$\frac{ds_z^2}{d\tau} \approx (Nar_H)\frac{\ln\Lambda_p}{ss_z} + s_z^2\mathcal{M}^{1/3}, \tag{16}$$

$$\frac{d\mathcal{M}}{d\tau} \approx p(Nar_H)\frac{\mathcal{M}}{s_z}. \tag{17}$$

In the dispersion-dominated regime ($s \gtrsim \mathcal{M}^{1/3}$)

$$\frac{d}{d\tau}\left(s^2, s_z^2\right) \approx (Nar_H)\frac{\ln\Lambda_p}{ss_z} + \mathcal{M}^2\frac{\ln\Lambda_e}{s^2 s_z}, \tag{18}$$

$$\frac{d\mathcal{M}}{d\tau} \approx p(Nar_H)\frac{\mathcal{M}^{4/3}}{ss_z}. \tag{19}$$

The different factors entering the Coulomb logarithms are

$$\Lambda_p = s^2 s_z \quad \text{and} \quad \Lambda_e = s^2 s_z/\mathcal{M}. \tag{20}$$

In the equations of evolution of s and s_z (15), (16), and (18) the first term on the r.h.s. describes the effect of planetesimal-planetesimal scattering while the last one accounts for the embryo-planetesimal encounters. We have dropped all numerical factors entering these equations because our qualitative analysis cannot determine them. However this should not affect our general conclusions.

We do not write down an equation of evolution for N — the surface density of planetesimals. Instead we simply assume it to be constant. This is certainly justified while the embryo's mass is small and it cannot perturb the spatial distribution of planetesimal orbits around it. However as it grows bigger, the embryo starts repelling planetesimals (Papers I & III) which affects their surface density. This effect is not included in our approach. It is often argued that the conservation of the Jacobi constant of planetesimals in the course of their scattering by the embryo can maintain their instantaneous surface density (which matters for the accretion) at more or less constant level; unfortunately it will turn out (see §3) that this assumption is not very good for very large embryo masses and more accurate treatment of evolution of N is required. However, this disadvantage of the assumption $N = const$ does not affect our major conclusions.

More accurate analysis shows that as well as the heating terms the equations for the planetesimal velocity evolution should also contain transport terms. These appear because mutual gravitational scattering of planetesimals acts as a source of effective viscosity in the disk (Papers I & II; Ohtsuki & Tanaka 2002) which tends to smooth out any inhomogeneities of planetesimal surface density and velocity dispersions. Equations (15)-(18) do not take this effect into account but this does not degrade the accuracy of our conclusions: it follows from our analysis of planetesimal-planetesimal scattering in Paper II that the transport (or viscous) terms lead to the effects of the same magnitude as the planetesimal heating terms. We will discuss this issue in more detail in §4.

The system (15)-(20) describes the dynamics of the disk only in the immediate vicinity of the embryo — within $\sim R_H$ from the embryo's orbit in the shear-dominated regime and within $\sim sR_H/\mathcal{M}^{1/3}$ in the dispersion-dominated regime. We will call this region the *"heated" zone*. Only

the dynamics of this region matters for the embryo's growth because embryo can accrete material only from this part of the disk. Outside the heated region, the embryo's influence is negligible and disk evolution proceeds almost exclusively under the action of planetesimal-planetesimal scattering. Evolution of the distant parts of the disk is described by equation (18) with the last term in its r.h.s. dropped and is rather simple.

One can easily see that the evolution equations incorporate only two free parameters characterizing disk properties: Nar_H and p. What is more important, the more accurate equations derived previously in Papers II & III also exhibit this property (see §3 and Appendix A). This implies that various evolutionary scenarios describing the growth of the embryo can be classified completely by these two parameters. After such classification is performed the general features of the evolution can be predicted once the values of the parameters Nar_H and p are known. Typical values of these parameters in MMSN are discussed later in §3.

Our subsequent analysis of equations (15)-(19) will be essentially asymptotic: we will separate the embryo-disk evolution into a sequence of regimes in which only some terms in the evolution equations are important. Evolution in the transition zones between separate asymptotic regimes will be neglected. The unimportance of the transient stages typically requires the changes of various quantities in asymptotic regimes to be much larger than in the transition zones. We will see that this is usually true only when extreme values of parameters Nar_H and p are chosen. However, even for a realistic choice of these parameters typical for MMSN our analysis will still give us important insight into the coupled evolution of the embryo-disk system.

2.2. Separation of the velocity evolution regimes.

Planetesimal-planetesimal scattering dominates the evolution of the planetesimal velocity when the first term in the r.h.s. of the corresponding equation exceeds the second term representing the effect of the embryo-planetesimal scattering. The shear-dominated regime corresponds to $\mathcal{M} > s^3$ in $s - \mathcal{M}$ coordinates. One can see from (15) that in this regime mutual planetesimal encounters dominate the growth of s and s_z when

$$\mathcal{M} < \mathcal{M}_{sd}(s) \approx \ln \Lambda_p \frac{Nar_H}{s^2}. \tag{21}$$

In writing down this condition we have assumed that $s \sim s_z$ which is always the case for three-dimensional scattering characterizing planetesimal-planetesimal encounters. Note that when $s \sim 1$, i.e. when even planetesimal-planetesimal scattering is close to the shear-dominated regime, the mass at which the embryo begins to dominate the disk dynamically is $M_e \sim m(Nar_H)$ [$\ln \Lambda_p \sim 1$ when $s, s_z \sim 1$, see (20)]. The same estimate of M_e was obtained in Paper I where both mutual planetesimal and embryo-planetesimal encounters were treated in the shear-dominated regime.

The dispersion-dominated regime occurs when $\mathcal{M} < s^3$. In this case the disk dominates its

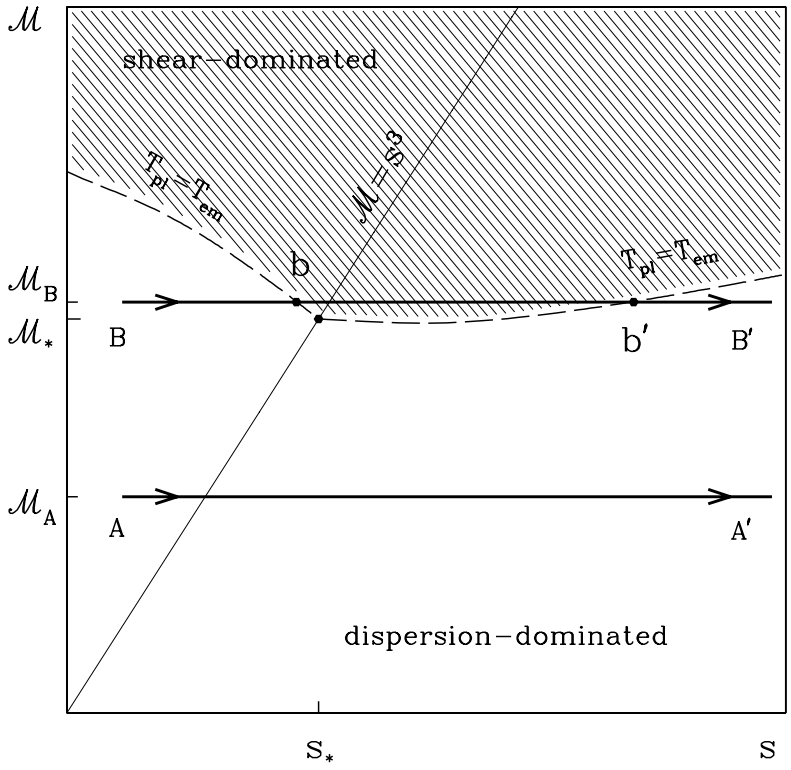

Fig. 1.— Different regions of embryo-planetesimal interactions, in coordinates $s = v/(\Omega r_H)$ and $\mathcal{M} = M_e/m$ [see equation (14)]. The thin solid line separates shear- and dispersion-dominated regimes, while the dashed curve separates regions where either embryo or planetesimals dominate disk heating [see equations (21) and (22); deep in the dispersion-dominated regime it has a slope of 1/2]. The embryo controls the disk evolution in the shaded region, mutual planetesimal scattering dominates disk evolution in the unshaded region. Two typical evolutionary tracks for an embryo of fixed mass are displayed: for $\mathcal{M}_A < \mathcal{M}_\star$ and for $\mathcal{M}_B > \mathcal{M}_\star$.

own dynamical evolution only when [see (18)]

$$\mathcal{M} < \mathcal{M}_{dd}(s) \approx \left(\frac{\ln \Lambda_p}{\ln \Lambda_e}\right)^{1/2} (Nar_H)^{1/2} s^{1/2}. \tag{22}$$

A similar condition (but without $\ln \Lambda_e$) was previously derived by Ohtsuki & Tanaka (2002).

Conditions (21) and (22) separate the s-$\mathcal{M}$ plane into regions where disk self-heating dominates over the effect of the embryo, and vice versa. These regions are displayed in Figure 1 and the one where embryo controls the disk heating is shaded. The curves in the s-$\mathcal{M}$ plane given by (21) and (22) intersect with each other and with $\mathcal{M} = s^3$ at the point $(s_\star, \mathcal{M}_\star)$ where

$$\mathcal{M}_\star \approx (\ln \Lambda_p)^{3/5} (Nar_H)^{3/5}, \quad s_\star \approx (\ln \Lambda_p)^{1/5} (Nar_H)^{1/5} = \mathcal{M}_\star^{1/3}, \quad \Lambda_p \approx (Nar_H)^{3/5}, \tag{23}$$

where we have taken into account that $\ln\Lambda_e \approx 1$ when $s, s_z \sim \mathcal{M}^{1/3}$, corresponding to the transition between the shear- and dispersion-dominated regimes [see (20)].

Let us assume initially that the embryo's mass does not evolve and the disk is initially in the shear-dominated regime. Since the disk can only heat up, the evolutionary track of the embryo-disk system in the s-$\mathcal{M}$ plane is a straight line going to the right at constant $\mathcal{M}$. It then follows from Figure 1 that when $\mathcal{M} < \mathcal{M}_\star$, the embryo can never be effective at heating the disk up and the evolution of eccentricities and inclinations of planetesimals takes place only as a result of planetesimal-planetesimal gravitational scattering — the effect of the embryo-planetesimal interaction is much weaker (evolutionary track A-A$'$ in Figure 1). On the contrary, when $\mathcal{M} > \mathcal{M}_\star$ (track B-B$'$ in Figure 1) embryo will start dominating the dynamical evolution of the heated zone when the disk is sufficiently excited in the shear-dominated regime (at point b). As the heated zone gets more and more excited (s grows) mutual planetesimal scattering starts eventually to dominate the disk evolution again (at point b'). This is actually not surprising because one can see from (18) that in the dispersion-dominated regime the embryo's contribution to the disk evolution scales roughly as s^{-3} while that of the mutual planetesimal encounters behaves as s^{-2} at a fixed $\mathcal{M}$. Thus, as s increases planetesimal encounters finally take over the control over the disk evolution in the heated region from the embryo. It would however take a very long time for the system to reach the transition point b' because usually $s_{b'} \gg 1$ and disk random motion evolution is very slow in the dispersion-dominated regime. We will not discuss any other details of the disk dynamical evolution with fixed $\mathcal{M}$ because realistic embryos have $p \neq 0$ and their masses have to increase.

2.3. Separation of the mass and velocity evolution regimes.

Whenever the mass of the embryo is allowed to vary one has to study the coupled embryo-disk evolution using the full set of equations (15)-(17) or (18)-(19). We will concentrate here on exploring the dispersion-dominated regime (we briefly touch on the shear-dominated regime in the end of this section).

Let us estimate different timescales associated with the evolution in the dispersion-dominated regime. Since $s_z \sim s$, the timescale of disk evolution caused by planetesimal-planetesimal scattering is [first term on the r.h.s. of (18)]

$$T_{pl} = \left(\frac{1}{s}\frac{ds}{d\tau}\Big|_{pl}\right)^{-1} \approx \frac{s^4}{\ln\Lambda_p}\frac{1}{Nar_H}. \tag{24}$$

The timescale characterizing the effects of the embryo is given by [last term on the r.h.s. of (18)]

$$T_{em} = \left(\frac{1}{s}\frac{ds}{d\tau}\Big|_{em}\right)^{-1} \approx \frac{s^5}{\ln\Lambda_e}\frac{1}{\mathcal{M}^2}. \tag{25}$$

Finally the characteristic time of the embryo's mass growth is

$$T_M = \left(\frac{1}{\mathcal{M}}\frac{d\mathcal{M}}{d\tau}\right)^{-1} \approx \frac{s^2}{\mathcal{M}^{1/3}}\frac{1}{p(Nar_H)}. \tag{26}$$

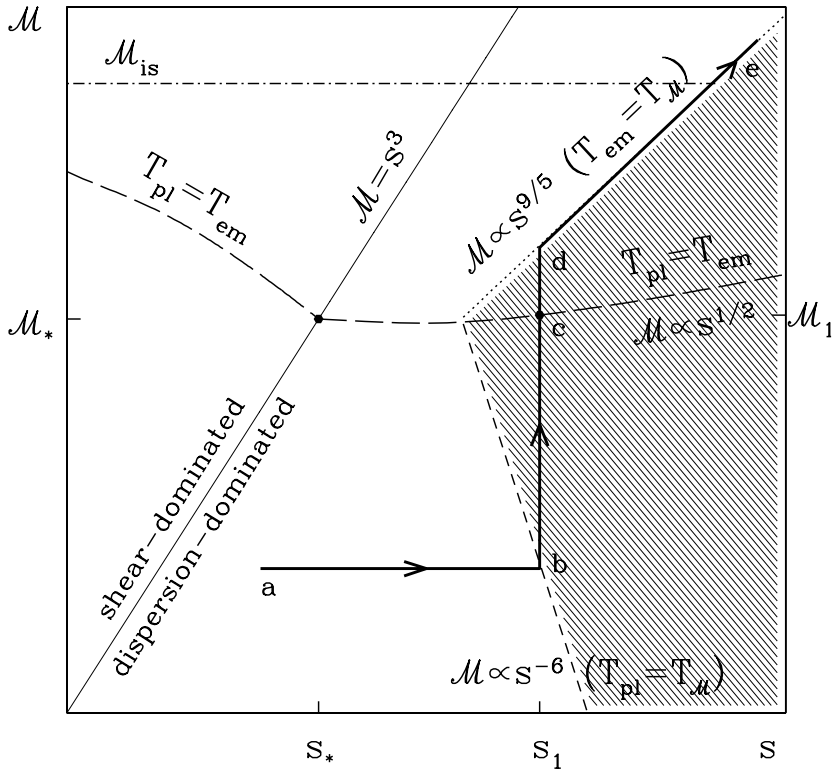

Fig. 2.— Separation of different regions in the s-$\mathcal{M}$ space [see equation (14)] in the case of coupled evolution of disk velocity dispersion and embryo's mass. The dotted line displays the asymptotic relation (28) and the short-dashed line shows relation (27). The dot-dashed line represents the restriction put by the existence of the isolation mass [see (38) in §3.1]. The embryo's mass evolves faster than the disk velocity dispersion in the shaded region (and vice versa in the unshaded region). The thick solid curve shows typical evolutionary track of the embryo-disk system. The long-dashed curve has the same meaning as in Figure 1 (its slope is 1/2 when $s \gg \mathcal{M}^{1/3}$).

By requiring $T_{pl} = T_{em}$ we retrieve the separation condition (22) again.

Let us assume that at the beginning embryo has mass $\mathcal{M} < \mathcal{M}_\star$ [$\mathcal{M}_\star$ is given by equation (23)]. Then initially disk evolution is dominated by planetesimal-planetesimal scattering. The disk evolves faster than M_e grows only when $T_{pl} \leq T_M$ or when (see Figure 2)

$$\mathcal{M} \leq \mathcal{M}_{M-pl}(s) \approx \left(\frac{\ln \Lambda_p}{p}\right)^3 \frac{1}{s^6}. \tag{27}$$

When $\mathcal{M}$ grows bigger than $\mathcal{M}_{dd}$ given by (22), the embryo starts dominating the velocity evolution of the disk in the heated zone. This evolution proceeds faster than the embryo's mass grows when $T_{em} \leq T_M$ or

$$\mathcal{M} \geq \mathcal{M}_{M-em}(s) \approx \left[\frac{p(Nar_H)}{\ln \Lambda_e}\right]^{3/5} s^{9/5}. \tag{28}$$

The curves in the s-$\mathcal{M}$ plane given by equations (27) and (28) intersect with each other and with (22) in the dispersion-dominated regime (when $s \geq \mathcal{M}^{1/3}$) if $p > p_0$, where

$$p_0 \approx \frac{(\ln \Lambda_p)^{2/5}}{(Nar_H)^{3/5}}. \tag{29}$$

Thus, when $p > p_0$ there is a region in the dispersion-dominated regime bounded by curves (27) and (28) in which the embryo's mass grows faster than the random energy in the heated zone (shaded region in Figure 2). Everywhere outside this region the disk heats up faster than the embryo grows. This allows us to sketch the evolution of the system in the following way (thick solid curve $a - e$ in Figure 2) starting with some $\mathcal{M}_0 < \mathcal{M}_{M-pl}$: initially the disk heats up faster than $\mathcal{M}$ grows which produces an almost horizontal track $a - b$ in the s-$\mathcal{M}$ plane — see Figure 2. As s gets to the point b where $\mathcal{M}_0 \approx \mathcal{M}_{M-pl}$, mass starts growing faster than s; as a result the evolution track becomes almost vertical ($b-d$). At point c when the condition $\mathcal{M} = \mathcal{M}_{dd}$ [see (22)] is fulfilled, the embryo takes control over the dynamical evolution of the heated zone but its mass still grows faster than s increases [$T_M < T_{em}$, see (25) and (26)]. This continues until evolutionary track reaches the curve $\mathcal{M} = \mathcal{M}_{M-em}$ at point d. At this point timescales of the embryo's growth and disk dynamical evolution become almost equal and embryo-disk system evolves stably along the curve $d - e$.

This general picture is confirmed by the solution of the system (18)-(19). When $\mathcal{M} < \mathcal{M}_{dd}$ and planetesimal-planetesimal encounters dominate the disk heating one finds that (treating logarithmic factors as constants)

$$s(\tau) \approx [(Nar_H) \ln \Lambda_p]^{1/4} \tau^{1/4}, \qquad \mathcal{M}(\tau) \approx \mathcal{M}_0 \left[1 - (\tau/\tau_{run})^{1/2}\right]^{-3}, \tag{30}$$

where

$$\tau_{run} \approx \frac{\ln \Lambda_p}{\mathcal{M}_0^{2/3} (Nar_H) p^2} \tag{31}$$

is the timescale of the runaway growth. One can see from this solution that when the embryo is not massive enough to affect the disk dynamics around it does grow in the runaway regime which is in complete agreement with the scenario of Wetherill & Stewart (1989, 1993). However, in practice the runaway solution (30) is only valid until $\mathcal{M}(\tau) \approx \mathcal{M}_{dd}$. This mass is reached when $\tau \approx \tau_{run}$ since typically $\mathcal{M}_{dd} \gg \mathcal{M}_0$. This means that embryo starts to dominate disk heating at (see Figure 2)

$$s_1 = s(\tau_{run}) \approx \left(\frac{\ln \Lambda_p}{p \mathcal{M}_0^{1/3}}\right)^{1/2}, \qquad \mathcal{M}_1 = \mathcal{M}_{dd}(s_1) \approx \left[\frac{(Nar_H)(\ln \Lambda_p)^{3/2}}{p^{1/2} \mathcal{M}_0^{1/6} \ln \Lambda_e}\right]^{1/2}. \tag{32}$$

After this happens evolution proceeds along a different route. One can find from (18)-(19) that for $\mathcal{M} \gg \mathcal{M}_1$ the evolutionary track is described by the equation

$$\mathcal{M} = \left[\mathcal{M}_1^{5/3} + \frac{p(Nar_H)}{\ln \Lambda_e}(s^3 - s_1^3)\right]^{3/5}. \tag{33}$$

Asymptotically, when $s \gg s_1$ this relationship reduces to (28) and one obtains that

$$s(\tau) \approx \frac{[p(Nar_H)]^{6/7}}{(\ln \Lambda_e)^{1/7}} \tau^{5/7}, \quad \mathcal{M}(\tau) \approx \frac{[p(Nar_H)]^{15/7}}{(\ln \Lambda_e)^{6/7}} \tau^{9/7}. \tag{34}$$

Note that this solution does not depend on $\mathcal{M}_0, \mathcal{M}_1, s_1$, etc. — all the memory of initial conditions is lost. For this reason we would expect *any* evolutionary track describing embryo-disk system to behave eventually as equation (34) predicts, independent of the initial conditions used.

The solutions of evolution equations obtained in this sections directly pertain only to the case $p < p_0$. If parameter p is such that $p > p_0$ the curves given by (27) and (28) do not intersect in the dispersion-dominated regime. As a result embryo-planetesimal system can in principle switch from this velocity regime to the shear-dominated or the intermediate velocity regime. We do not explicitly study the case $p > p_0$ in this paper — it turns out to be not very different from the case $p < p_0$ for the typical MMSN parameters (see §3). We also do not derive any results for the embryo-disk evolution in the shear-dominated regime. There are several reasons for this:

- One would expect that initial disk velocity dispersion and starting mass of the embryo are correlated with each other since both require some time to grow; this is likely to bring the system into the dispersion-dominated rather than shear-dominated regime.
- For the parameters typical for MMSN the variation of s in the shear-dominated regime is restricted to a rather narrow range. It is thus possible that the asymptotic analysis such as presented in §2.2 and §2.3 would not be very helpful in this case since the effects of the transition zones between the different asymptotic regimes will be quite important (see discussion in the end of §2.1). This is even more important for the case $p > p_0$.
- It is unlikely that the embryo-disk system can spend a long time in the shear-dominated regime since the dynamical evolution of the disk is usually very rapid in this case. Thus the shear-dominated evolution is expected to be only a transient stage of the system's history.
- The numerical approach we are going to use for the description of the embryo-planetesimal interaction is not very accurate in the shear-dominated regime (see Paper III).

These arguments provide the basis for our present neglect of the shear-dominated and intermediate velocity stages of the embryo-disk evolution. However it is clearly not difficult to study these regimes qualitatively based on equations (15)-(17) in the spirit of §2.2 and §2.3 if the need arises.

3. Numerical results.

One can study the embryo-disk interaction and check the simple qualitative predictions of §2 using more robust machinery. To do this we use the apparatus elaborated in Papers II & III for

the statistical description of the planetesimal-planetesimal and embryo-planetesimal gravitational scattering. There we have derived a set of equations governing self-consistently both the planetesimal disk dynamics and the embryo's mass growth, taking into account planetesimal-planetesimal as well as embryo-planetesimal gravitational scattering. These equations are the most accurate when the embryo-planetesimal interaction is in the dispersion-dominated regime although we are able to provide an approximate treatment of the intermediate velocity regime as well (see Paper III). In Appendix A we transform this set of equations into a dimensionless form. We then numerically solve them and find the embryo's mass as a function of time; in addition we obtain time-dependent and spatially-resolved profiles of the planetesimal surface density and dispersions of eccentricity and inclination. What makes this analysis novel is that it takes into account the effects of planetesimal disk nonuniformities induced by the embryo's gravity. The closest existing analog of our method is a multi-zone coagulation simulation approach of Spaute *et al.* (1991) and Weidenschilling *et al.* (1997) which achieves spatial resolution by employing a large number of single-zone coagulation simulations interacting through the boundaries. However in their published simulations the treatment of the disk dynamical evolution is very rough and the degree of the spatial resolution is not very large — of the order of Hill radii of biggest bodies at best while our approach allows us to use much smaller grid sizes.

3.1. Numerical setup.

In this paper we are interested in the growth of a single isolated embryo. We assume a planetesimal population with a single characteristic mass and disregard the evolution of this mass due to the planetesimal coagulation. We neglect any mechanisms which can affect planetesimal dynamics (gas drag, inelastic collisions, etc.) other than gravitational scattering. The embryo's eccentricity and inclination are assumed to be always zero. We are going to relax these assumptions in future work. As the embryo's mass increases, its Hill radius R_H (which is a characteristic length scale of the problem) grows as well. For this reason we compute the spatial distributions of various quantities not in the physical coordinates but in Hill coordinates of the embryo which naturally adjust to the embryo's mass growth. For the same reason in our numerical calculations we characterize the dynamical state of planetesimal disk not by s and s_z defined by (14) but by S and S_z — velocity dispersions in horizontal and vertical directions normalized by the embryo's Hill radius R_H (and not by the planetesimal Hill radius r_H):

$$S^2 = \frac{\langle v^2 \rangle}{(\Omega R_H)^2} = \frac{\sigma_e^2}{\mu_e^{2/3}} = \frac{s^2}{\mathcal{M}^{2/3}}, \quad S_z^2 = \frac{\langle v_z^2 \rangle}{(\Omega R_H)^2} = \frac{\sigma_i^2}{\mu_e^{2/3}} = \frac{s_z^2}{\mathcal{M}^{2/3}}, \tag{35}$$

where σ_e and σ_i are the (nonreduced) eccentricity and inclination dispersions of Paper II. When making comparisons with §2 we usually switch back to variables s and s_z. The dimensionless variables $\mathcal{M}$ and τ defined in equation (14) are used instead of the embryo's mass and time. The width of the integration region in Hill coordinates is chosen to be large enough [usually $(-40R_H; 40R_H)$ in coordinates which adjust to the embryo's mass] so as to minimize boundary effects.

To provide an estimate of the random velocity dispersion s in the heated zone (which is one of the functions of interest) in our numerical solutions we have chosen the following method: we determine the extent of the region around the embryo within which the excess of eccentricity dispersion over its value at infinity is $> 20\%$ of the maximum value of this excess. We define this to be the heated zone. Then we average $(S^2 + S_z^2)^{1/2}$ over this region and use the resultant quantity [multiplied by $\mathcal{M}^{2/3}$, see (35)] as a measure of planetesimal random velocity s. At this point we do not make a distinction between the total velocity $\sqrt{s^2 + s_z^2}$ and its horizontal component s because they are approximately the same at our level of accuracy. This is rather loose definition of s but it suffices for our purposes.

As we have already mentioned in §2.1 the outcome of the embryo and planetesimal disk evolution depends only on the values of Nar_H and p. This simplifies our treatment a lot by combining several different quantities (such as m, a, N, M_c, etc.) into just two parameters. The parameter Nar_H has the meaning of (roughly) the number of planetesimals within the annulus of width r_H and radius equal to the embryo's semimajor axis a. This number is typically quite large. Parameter p is simply the ratio of the physical size of the body to its Hill radius. Since both radii depend on the mass of the body in the same way (both are $\propto M_e^{1/3}$) p is actually independent of M_e and can be taken to characterize both the embryo and planetesimals. In many astrophysically relevant situations this parameter is small. Using MMSN parameters given by (5) we can estimate that

$$Nar_H = \frac{\Sigma a^2}{m^{2/3} M_c^{1/3}} \approx 360 \left(\frac{a}{1\ \mathrm{AU}}\right)^{1/2} \left(\frac{10^{21}\ \mathrm{g}}{m}\right)^{2/3} \left(\frac{M_\odot}{M_c}\right)^{1/3} \tag{36}$$

and

$$p = \left(\frac{3}{4\pi}\frac{M_c}{\rho a^3}\right)^{1/3} \approx 3.6 \times 10^{-3} \left(\frac{1\ \mathrm{AU}}{a}\right) \left(\frac{3\ \mathrm{g\ cm^{-3}}}{\rho}\right)^{1/3} \left(\frac{M_c}{M_\odot}\right)^{1/3}, \tag{37}$$

where ρ is the density of solid material constituting planetesimals as well as the embryo. In Table 1 one can find typical values of these parameters in different important locations of the protosolar

Table 1. Typical values of Nar_H and p.[1]

Typical object	a, AU	Nar_H ($m = 10^{21}$ g)	p
Earth	1	360	3.6×10^{-3}
Jupiter core	5	800	7×10^{-4}
KBO	40	2.3×10^3	0.9×10^{-4}

[1]In computing these values $M_c = M_\odot$ and $\rho = 3$ g cm^{-3} are used.

nebula. Note that for a given ρ and M_c equation (37) unambiguously determines the semimajor axis in the MMSN corresponding to a particular value of p. Knowledge of Nar_H then allows one to fix the planetesimal mass m.

We numerically solve the evolution equations of Appendix A and compare the results with the predictions of §2. We display the outcomes of calculations for 3 representative cases: $Nar_H = 400, p = 0.004$ corresponding to $a = 0.9$ AU and $m = 7.3 \times 10^{20}$ g which is typical for the terrestrial planet region; $Nar_H = 10^3, p = 10^{-3}$ ($a = 3.6$ AU and $m = 1.5 \times 10^{21}$ g) which is close to the region of giant planet formation; $Nar_H = 10^3, p = 10^{-4}$ ($a = 36$ AU and $m = 4.7 \times 10^{22}$ g) which is representative of the distant part of the protosolar nebula where Kuiper Belt Objects (KBOs) are assumed to form (although the typical planetesimal mass is almost certainly too big in this case). In each case the calculation was carried out for several values of initial embryo's mass $\mathcal{M}_0$ and velocity dispersion s_0 (which is usually unimportant). Each calculation starts with a protoplanetary embryo in a homogeneous disk; we follow both the subsequent growth of embryo's mass and the development of disk inhomogeneities.

We allow the disk-embryo system to evolve until $\mathcal{M}$ exceeds the restriction put by the existence of the isolation mass M_{is} (for higher masses our results are not accurate because planetesimal surface density would be considerably reduced by accretion). From the definition of M_{is} (see §1) it follows that[4] $M_{is} \approx 2\pi a \times 2a(M_{is}/M_c)^{1/3} mN$, or in our dimensionless notation

$$\mathcal{M}_{is} \simeq (4\pi)^{3/2} (Nar_H)^{3/2}. \tag{38}$$

In fact, in the dispersion-dominated regime this condition should be additionally multiplied by $S^{3/2} = s^{3/2}/\mathcal{M}^{1/2}$ because in this velocity regime the width of the feeding zone is about the planetesimal epicyclic excursion SR_H. Thus, (38) should be considered a lower limit on the isolation mass which is valid in the shear-dominated regime only; in the dispersion-dominated regime the isolation mass becomes

$$\mathcal{M}_{is} \simeq 4\pi (Nar_H) s. \tag{39}$$

Obviously the more dynamically excited planetesimal disk is (i.e. the higher s is) the more massive the embryo can grow, because it can accrete planetesimals from a larger region of the nebula.

3.2. General description of evolution.

The results of the numerical solution of the evolution equations are presented in Figures 3-12. We use the following general notation when plotting evolutionary tracks of different quantities ($\mathcal{M}$ or s): tracks corresponding to the regime where planetesimal-planetesimal scattering dominates the disk dynamics are plotted in blue, while those in the regime dominated by embryo-planetesimal

[4]We assume here that the width of the feeding zone is $2R_H$ rather than R_H as has been assumed in Paper I.

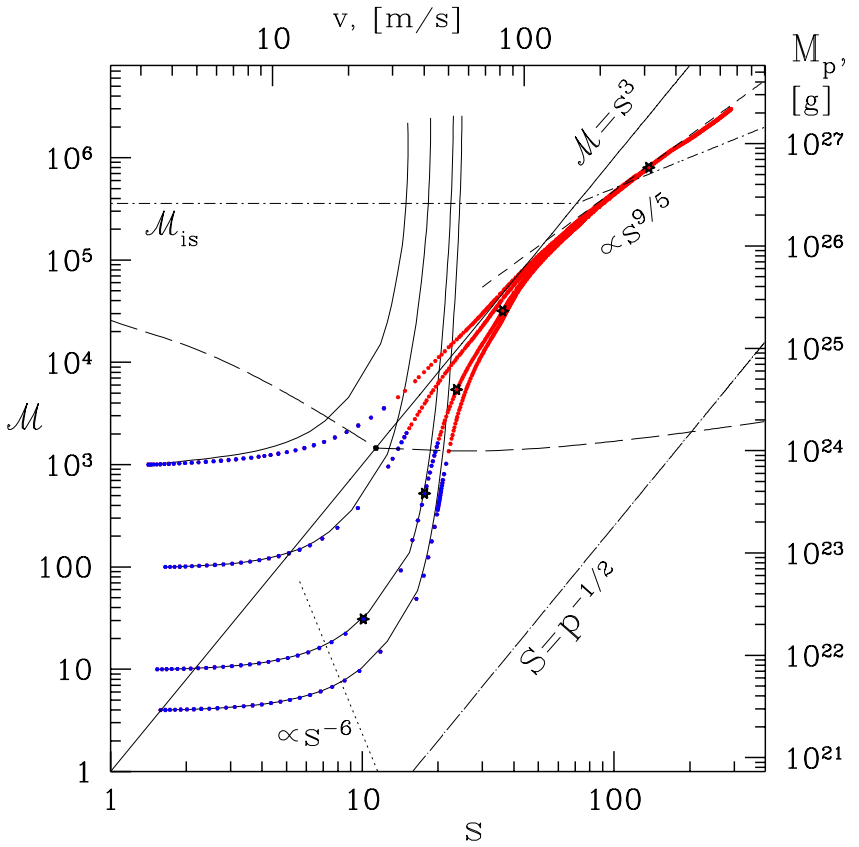

Fig. 3.— Evolution of the embryo-disk system in s-$\mathcal{M}$ coordinates for $Nar_H = 400$ and $p = 0.004$ (typical for the Earth-forming region of MMSN). The evolutionary tracks consist of two portions: where planetesimal scattering dominates the dynamical evolution of the disk (blue dots) and where embryo dominates this process (red dots). Curves separating various regions in this plot have the same meaning as in Figure 2. The thin solid curves initially coinciding with the dotted tracks describe the runaway growth of "passive" embryos.

scattering are shown with red. The separation between these two regimes is determined based on Figures 10-12 (see below). We also plot on each Figure (on the right and top borders) the numerical values of physical variables M_e (mass of the embryo) and v (linear velocity of planetesimal epicyclic motion) corresponding to their dimensionless analogs $\mathcal{M}$ and s. In doing this we take into account the aforementioned property [see discussion after (36) and (37) of Nar_H and p to unambiguously specify a and m when ρ and M_c are fixed. Also, where appropriate we plot not only the evolutionary tracks including the effects of embryo's gravity on the disk dynamics ("active" embryo, colored dots) but also the curves calculated assuming that embryo does not affect the disk dynamics (thin solid lines); in other words we allow the disk to stay completely homogeneous and to heat up only due to the planetesimal-planetesimal scattering, while still allowing the embryo to grow ("passive" embryo). This would correspond to the outcome of conventional coagulation simulations (in our problem setting) which do not take embryo-induced disk inhomogeneities into account.

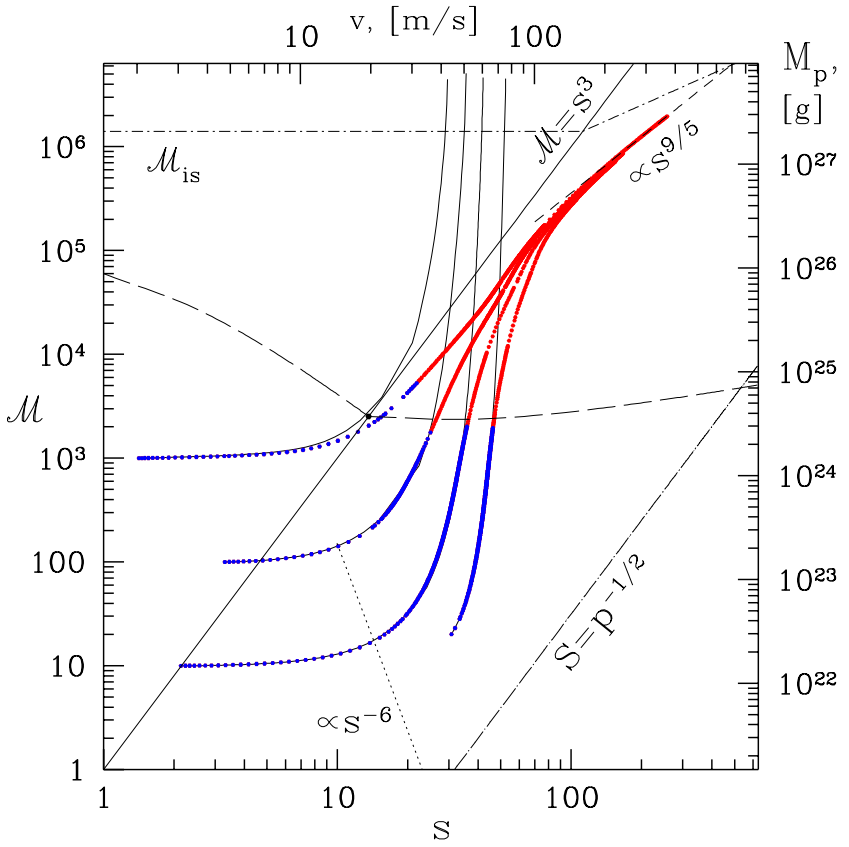

Fig. 4.— The same as Figure 3 but for $Nar_H = 10^3$ and $p = 10^{-3}$ (typical for the Jupiter-forming region of MMSN).

In Figures 3-5 we plot the evolution of the embryo-disk system in coordinates s-$\mathcal{M}$ for different values of Nar_H and p. This can be compared to the schematic calculations in Figure 2. Each of the plots displays several evolutionary tracks shown by sequences of dots. These tracks usually start with moderate values of $\mathcal{M}_0$ (from 10 to 10^3) and rather small values of s_0, so that the embryo-disk interaction can start either in the shear- or in the dispersion-dominated regimes. A brief inspection of Figures 3-5 shows that the coupled evolution of the embryo-disk system can be naturally split into three distinct regimes. In the first regime the mass of the embryo stays almost constant[5] and only the velocity dispersion in the disk grows. After a short intermediate stage when both s and $\mathcal{M}$ evolve at comparable rates, the embryo grows faster than disk heats up because of the fast runaway accretion. At some intermediate point during this stage the embryo begins to dominate the dynamical evolution of the planetesimal disk (blue dots change to red dots). As a result the evolutionary track gradually departs from the runaway path and accretion proceeds at a slower rate. Finally, the system settles onto the asymptotic regime in which embryo's mass grows as a power law of the velocity dispersion in the heated zone s.

[5]This happens because the timescale of the runaway growth is longer than the timescale of the disk heating.

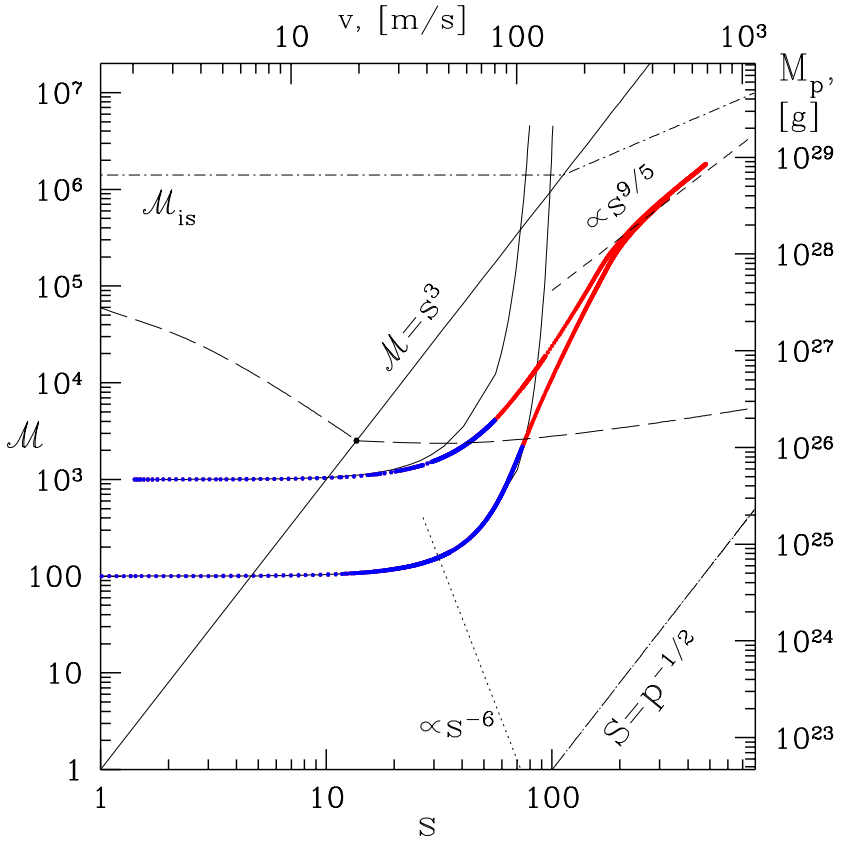

Fig. 5.— The same as Figure 3 but for $Nar_H = 10^3$ and $p = 10^{-4}$ (typical for the KBO-forming region of MMSN).

Figure 6 provides more insight into what is going on in the disk by plotting the time evolution of the spatial distributions of planetesimal surface density N and eccentricity and inclination dispersions S and S_z [scaled by R_H, see (35)]. These distributions are plotted for an evolutionary track with $Nar_H = 400, p = 0.004$ and initial values of mass and velocities $\mathcal{M}_0 = 10, S_0 = S_{z0} = 0.5$. We also plot the locations of the points at which the snapshots of spatial distributions are taken in Figures 3, 7, and 10 (black stars on the corresponding evolutionary track). One can see that initially the disk heats up very quickly: S grows from 0.5 to 2.8, S_z from 0.5 to 1.6 on a rather short timescale. The ratio of S_z/S is close to 0.55, which is characteristic for homogeneous Keplerian disks (Ida *et al.* 1993; Stewart & Ida 2000). One can see that the embryo's effects are negligible and disk is very uniform (red curve). After that rapid runaway accretion of the embryo leads to the decrease of S and S_z because growth of R_H surpasses the increase of s and s_z. Disk inhomogeneities are rather small while disk dynamics is still dominated by the mutual planetesimal encounters (blue curve). However, as soon as the embryo takes over the control of the disk heating (green curve) deviations from the uniform state become important: sharp features appear in the distributions of S and S_z and the embryo carves out a gap in surface density of planetesimal guiding centers around itself (results analogous to those of Papers I & III). After the intermediate stage (magenta curve), the disk finally settles into the asymptotic regime (black curve) and the difference between

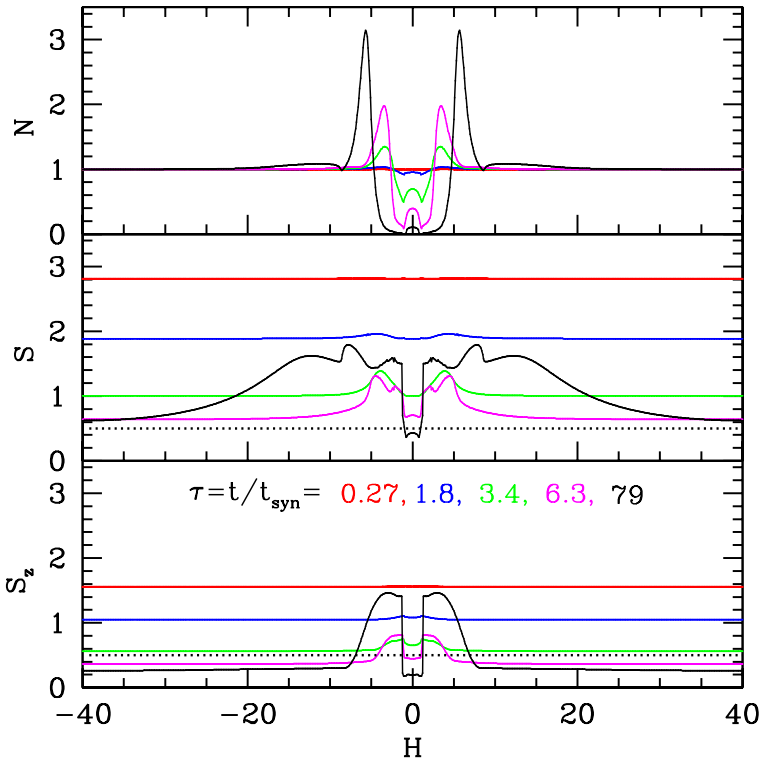

Fig. 6.— Time evolution of the spatial distributions of planetesimal surface density N (normalized by its value at infinity), eccentricity and inclination dispersions S and S_z scaled by the embryo's Hill radius for $Nar_H = 400, p = 0.004, \mathcal{M}_0 = 10, S_0 = 0.5, S_{z0} = 0.5$. Curves of different color represent the snapshots of the distributions at different moments of time marked with corresponding color (also marked on the evolutionary track in Figures 3, 7, & 10 with starred dots). The dotted line shows the initial state of the disk. See text for more details.

the planetesimal velocities in the heated zone and far from the embryo steadily grows with time. The detailed shapes of the spatial distributions of different quantities are almost invariant in the asymptotic regime — we would obtain the same final profiles if we were to start with a different set of $\mathcal{M}_0, S_{e0}, S_{i0}$. Note that far away from the embryo, the disk always stays uniform and S_z/S is always near 0.55[6].

It is interesting that for a rather long period of time disk evolution in the heated zone takes place almost in the shear-dominated regime. This happens because the runaway growth of the embryo's mass is much faster than the growth of random velocities in the disk. This switches embryo-planetesimal interactions from the dispersion-dominated into the intermediate velocity

[6]This ratio of S_z/S eventually falls in the very late stages of embryo-disk evolution, because eccentricity is rather effectively excited by the distant encounters (see e.g. Hasegawa & Nakazawa 1990).

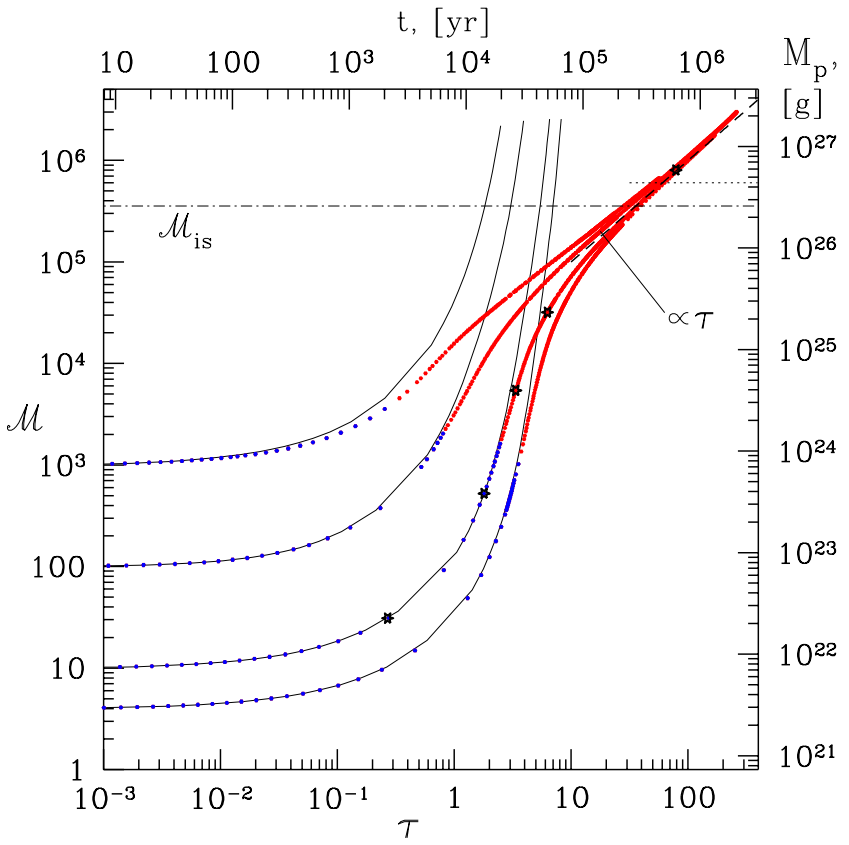

Fig. 7.— Growth of the embryo's mass in the case $Nar_H = 400$, $p = 0.004$ for different initial conditions. Mass $\mathcal{M}$ as a function of time τ is plotted by dots. The thin solid lines display corresponding runaway curves obtained by neglecting embryo's dynamical effects. The dimensional values of time t and mass of the embryo M_e are obtained in the same way as in Figures 3. The dot-dashed line represents the isolation mass in the shear-dominated regime defined by (38) and by (39) in the dispersion-dominated regime (see text). The dashed line has a slope of unity and shows the asymptotic behavior of $\mathcal{M}$ [see equation (45)].

regime. Some minor details of the spatial distributions in this regime might be not real because our analytical apparatus developed in Paper III is not very accurate in the intermediate velocity regime; however the overall description of the disk evolution should be robust.

We have mentioned in §2.3 that planetesimal-planetesimal scattering leads not only to the excitation of planetesimal random motions but also to the spatial redistribution of their kinetic energy and surface density (see also Paper II). This is equivalent to the action of the effective viscosity in the planetesimal disk which tries to smooth out the gradients of the surface density N and velocity dispersions S and S_z. As we have mentioned in §2.3 the magnitude of the effect produced by the viscosity is typically the same as that of the direct excitation of planetesimal velocities by planetesimal-planetesimal scattering. Planetesimal viscosity is very large initially when planetesimal velocities are small. As a result the spatial profiles of N, S and S_z are very

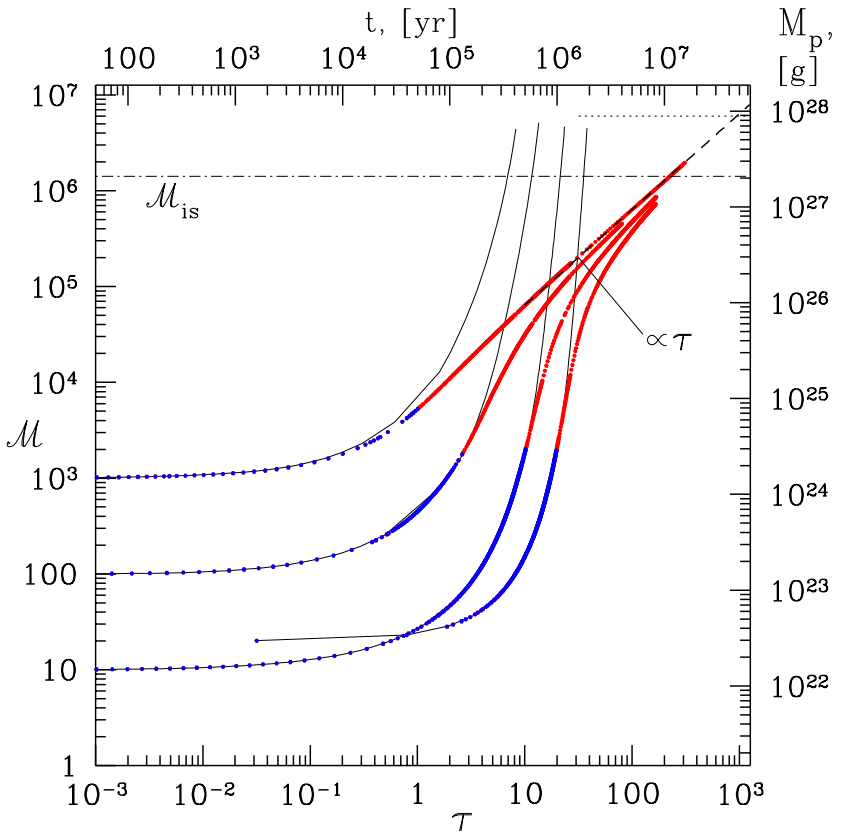

Fig. 8.— The same as Figure 7 but for $Nar_H = 10^3$, $p = 10^{-3}$.

smooth (red or blue curves). Later on gravitational effects of the embryo increase as well as the planetesimal velocities; this acts to diminish the role of viscosity — spatial distributions start to exhibit sharp features driven by the embryo's gravity (green and magenta curves). Finally, deep in the asymptotic regime (black curve) where s is very large viscosity is very small: it cannot even smooth out strong gradients of S and S_z at the edges of the region occupied by the planetesimals on the horseshoe orbits (planetesimal heating inside this zone is very weak). This justifies the validity of the concept of the "heated" zone: when embryo dominates nearby disk dynamics, the planetesimal viscosity which couples the excited region to the distant parts of the disk becomes relatively unimportant, and the heated region can be considered as dynamically isolated from the rest of the disk.

The general picture of the embryo-disk evolution outlined in Figures 3-6 is in excellent agreement with the predictions of our simple qualitative analysis presented in §2. We have attempted to provide some quantitative comparisons by fitting analytical results of 2.2 and 2.3 to the boundaries of various regions in Figures 3-5. For example, using the transition between the regions where embryo and planetesimals separately dominate the disk dynamics (where the color of the dots changes in our plots) we can estimate the approximate position of a critical point $(s_\star, \mathcal{M}_\star)$ defined by (23):

$$\mathcal{M}_\star \approx 40\ (Nar_H)^{3/5}, \quad s_\star \approx 3.4\ (Nar_H)^{1/5}. \tag{40}$$

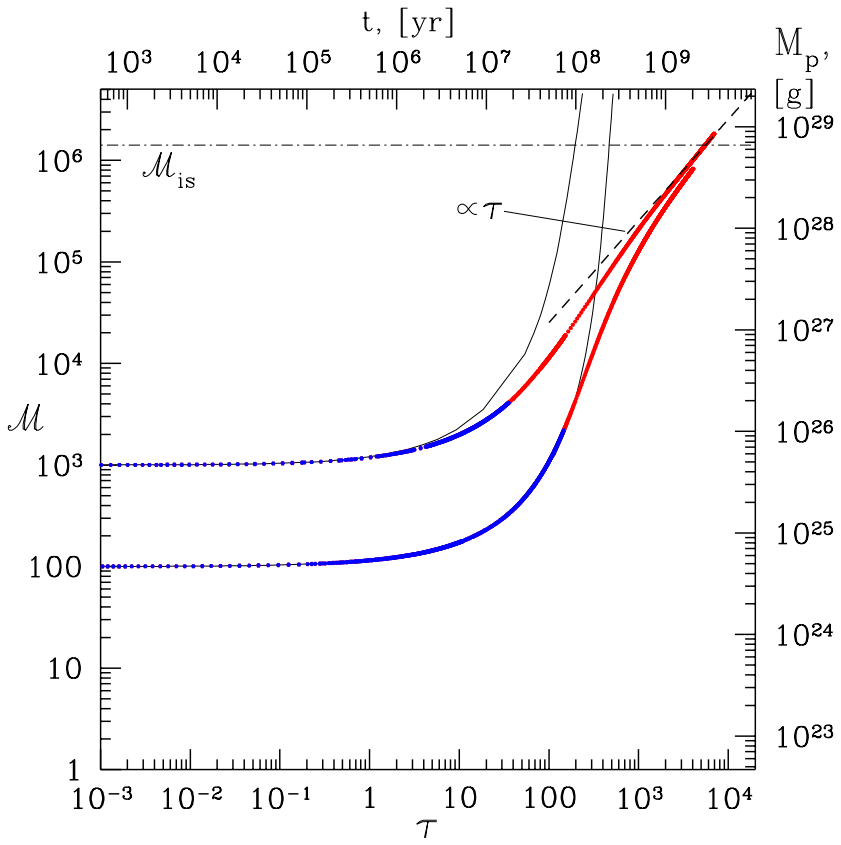

Fig. 9.— The same as Figure 7 but for $Nar_H = 10^3$, $p = 10^{-4}$.

In making this estimate we have neglected the variation of logarithmic factor with Nar_H and treated it as a constant which is absorbed in the coefficient in (40). We forced this point to lie on the line $\mathcal{M} = s^3$ (thin solid line) separating shear- and dispersion-dominated regimes of the embryo-planetesimal interaction. In the same spirit we have found that the position of the separatrix between the regions of planetesimal and embryo dominance over the disk dynamics $\mathcal{M}_{dd}(s)$ [see equation (22)] can be roughly fitted by

$$\mathcal{M}_{dd}(s) \approx \left[\frac{\mathcal{M}_\star^{5/3}}{\ln\Lambda_e}\right]^{1/2} s^{1/2}, \quad \Lambda_e = 1 + \frac{s^3}{\mathcal{M}_\star}. \tag{41}$$

This relation is shown by the long-dashed curve; one can see that within a factor of several it correctly predicts the transition from planetesimal to embryo's dominance of the disk dynamics although the agreement gets worse as one moves towards the shear-dominated regime [the continuation of this separatrix into the shear-dominated region is drawn using (21)]. We have kept the logarithmic dependence on s in (41) since it slightly improves agreement with the numerical results. Our estimate of $\mathcal{M}_{dd}$ agrees with the corresponding condition suggested by Ohtsuki & Tanaka (2002), see their equation (39). They have the same functional dependencies[7] and numerical

[7]Note that the estimate of Ohtsuki & Tanaka (2002) mistakenly lacks a factor $\ln\Lambda_e$ (meaning that embryo-

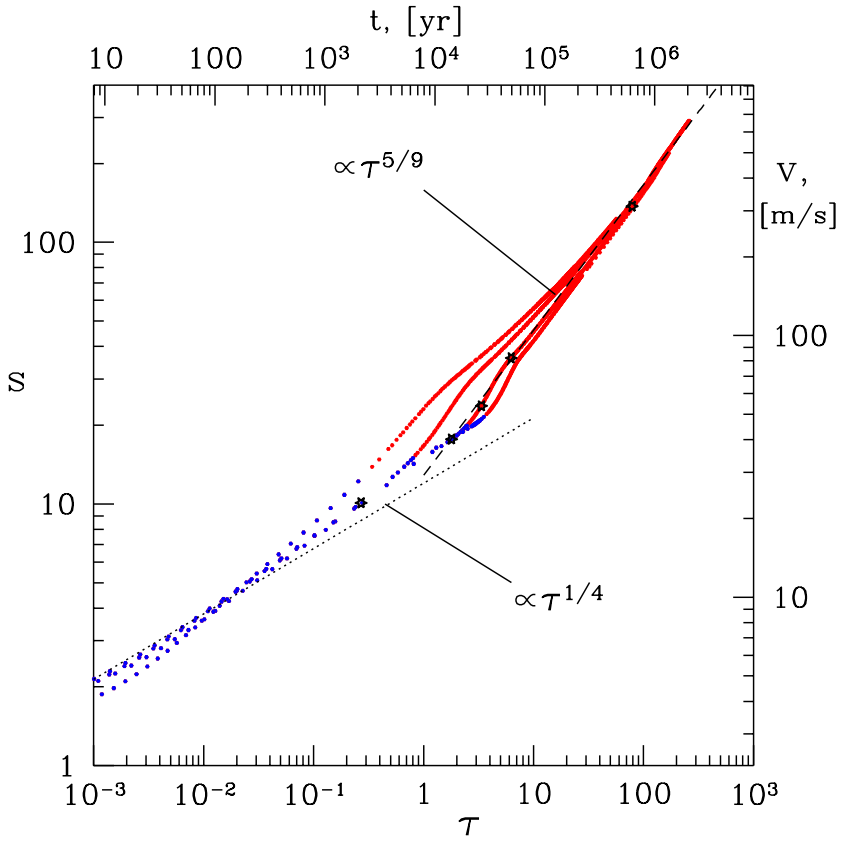

Fig. 10.— Growth of the disk velocity dispersion s in the heated zone as a function of time τ for $Nar_H = 400$, $p = 0.004$. Sequences of dots display $s(\tau)$ for different initial conditions. The dotted line has a slope of 1/4 and is intended to illustrate the initial growth of s due to the planetesimal-planetesimal scattering alone [see (30)]. The dashed line has a slope of 5/9 and shows the asymptotic behavior of s.

coefficients of the same order of magnitude.

One can see that the evolutionary tracks which were calculated without taking account of the embryo's effect on the disk dynamics (thin solid curves) coincide very well with those which include embryo's gravity while the disk evolution is dominated by planetesimal-planetesimal scattering. This is expected because when $\mathcal{M} < \mathcal{M}_{dd}$ the embryo cannot perturb the disk surface density or appreciably affect planetesimal velocities even in its own vicinity. As a result the disk stays homogeneous and heats up only by planetesimal encounters — exactly the situation for which the curves with a "passive" embryo were computed. However, as soon as the embryo takes over the control of the disk dynamics the evolutionary track with an "active" embryo departs from that of a "passive" embryo in agreement with equation (33): disk heating speeds up under the action of the embryo's gravity while the growth of embryo's mass slows down as a result of the

planetesimal interaction is in the dispersion-dominated regime) while still retaining $\ln \Lambda_e$.

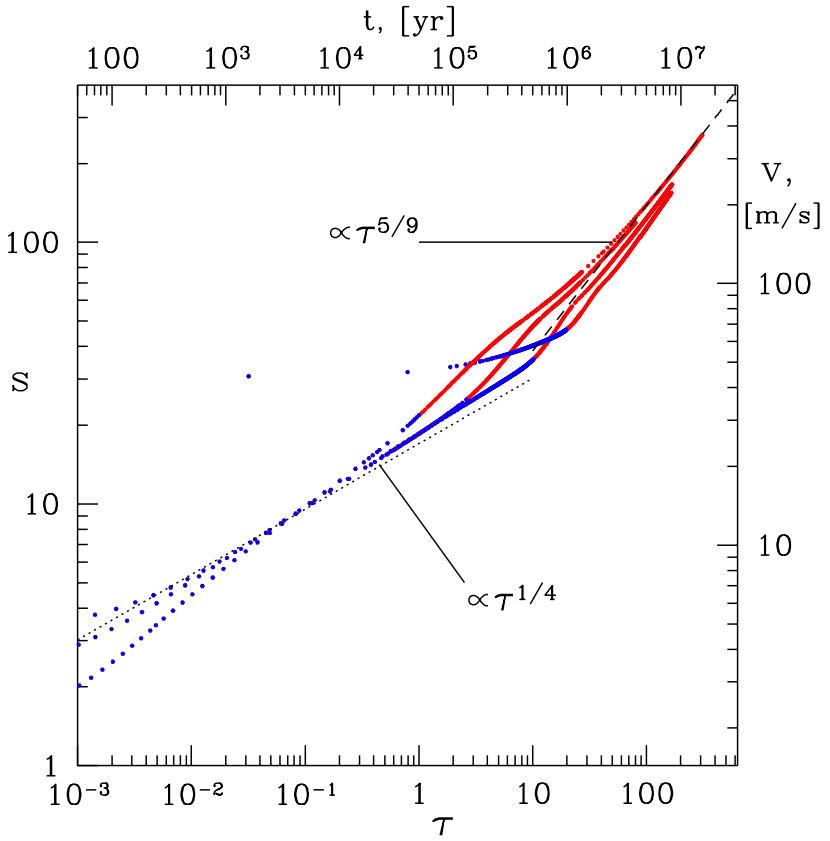

Fig. 11.— The same as Figure 7 but for $Nar_H = 10^3$, $p = 10^{-3}$.

weaker gravitational focussing of incoming planetesimals and, correspondingly, smaller collision cross-section.

Finally, in the late stages of its evolution the embryo-planetesimal system settles onto an attractor. There the dependence of $\mathcal{M}$ on s can be fitted by a power law with the index 9/5 [see equation (28)]. For a given Nar_H and p all evolutionary tracks independent of their starting $\mathcal{M}_0$ and s_0 end up on the same curve exactly as envisaged by our analysis in §2.3. Using numerical results for different Nar_H and p this curve can be approximated by [see (28)]

$$\mathcal{M}_{M-em}(s) \approx 90\ [p(Nar_H)]^{3/5} s^{9/5}. \tag{42}$$

This relation is shown by the short-dashed line in Figures 3-5. It is clearly an attractor to which all possible initial configurations finally converge. At some point this solution reaches the isolation mass $\mathcal{M}_{is}$ which is displayed by the short dash-dotted line — given by (38) in the shear-dominated regime and by (39) in the dispersion-dominated regime. It is important to stress that $\mathcal{M}_{is}$ is reached in the asymptotic regime of the embryo's evolution and not on the runaway stage. This has profound implications for the formation timescale of planetary embryos (see §4).

We have also checked the agreement between the predictions of §2.3 and our numerical results for the location of the separatrix between the regions where the embryo grows faster or slower than

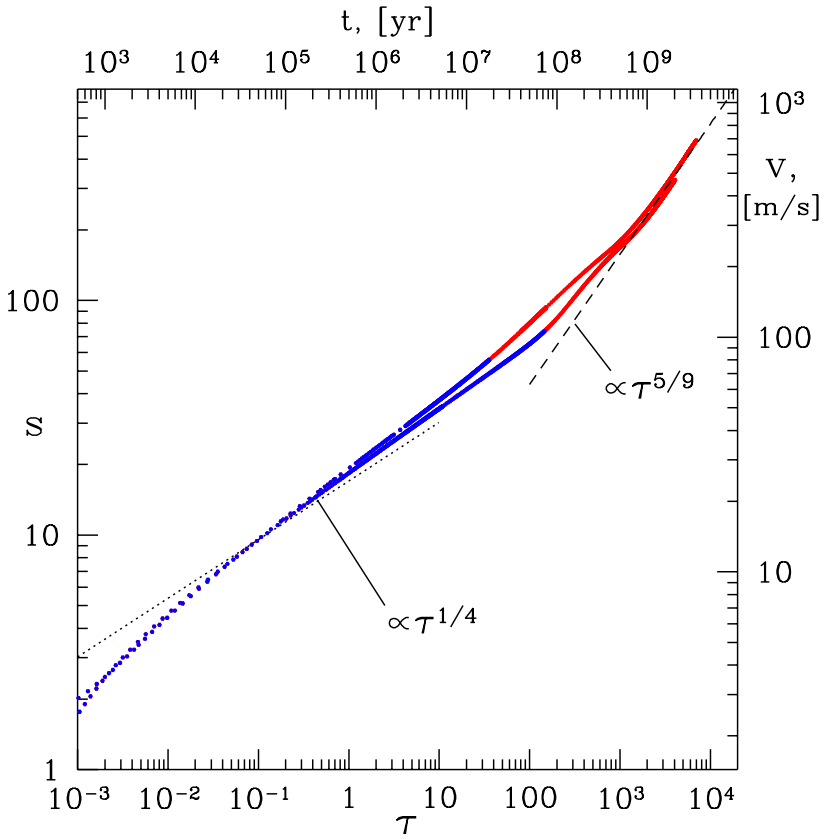

Fig. 12.— The same as Figure 7 but for $Nar_H = 10^3$, $p = 10^{-4}$.

planetesimals heat up the disk. This is the line where $\mathcal{M} = \mathcal{M}_{M-pl}(s)$ or $T_{pl} = T_{em}$ (see §2.3). In numerical calculations we set this transition at the point where the slope of evolutionary tracks in s-$\mathcal{M}$ coordinates is equal to 1, i.e. where $d\ln\mathcal{M}/d\ln s = 1$. The resulting curves for different Nar_H and p are well fitted by [see equation (27)]

$$\mathcal{M}_{M-pl}(s) \approx \frac{0.15}{(ps^2)^3}, \tag{43}$$

where the logarithmic factor $\ln\Lambda_e$ is again absorbed into a constant coefficient.

Note that the values of p and Nar_H we have used in our calculations typically do not lead to the crossing of $\mathcal{M}_{M-pl}(s)$ with $\mathcal{M}_{M-in}(s)$ in the dispersion-dominated regime [meaning that $p > p_0$, see equation (29)]. Nevertheless, our numerical results are still in good concord with the analytical results of §2.3 which were derived assuming that these curves do cross in the dispersion-dominated regime [i.e. $p < p_0$]. This is explained by the argument put forward in the end of §2.3: values of Nar_H and p that we have considered are not very extreme (Nar_H is not large enough and p is not small enough) and, as a result, evolutionary tracks do not explore regions of s-$\mathcal{M}$ space characteristic for the shear-dominated case. They only dwell for some time in the intermediate zones where transitions from one asymptotic regime to the other occur. Of course, if one were to explore e.g. larger values of Nar_H some differences from the case studied in §2.3 would appear.

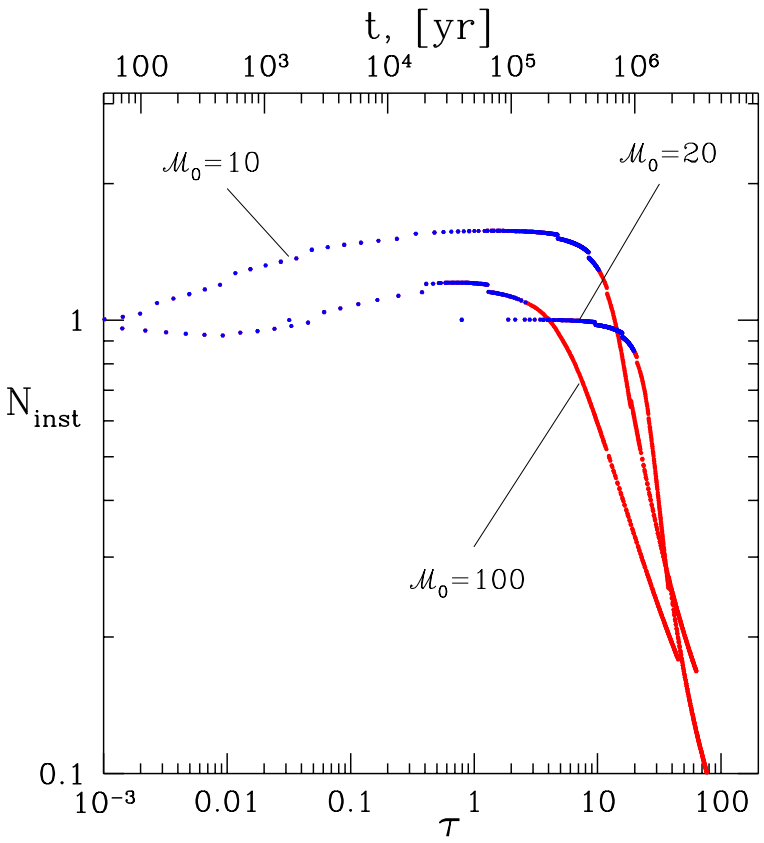

Fig. 13.— Instantaneous surface density of planetesimals which can be accreted by the embryo N_{inst} as a function of time. Curves for several different values of initial embryo's mass are shown (labeled on the figure). Note the sharp drop of N_{inst} after embryo starts to dominate the dynamics of the heated zone.

We expect though that this would not change our principal conclusions.

3.3. Time dependence of $\mathcal{M}$ and s.

In Figures 7-9 we plot the dependence of embryo's mass on time for the evolutionary tracks shown in Figures 3-5. Here one can see better that disk evolution with the "passive" embryo (thin solid curves) really leads to a runaway — mass of the embryo grows to extremely large values in a finite time. We have found that mass growth on this runaway stage can be approximately described by equation (30) with τ_{run} roughly (within a factor of 2) given by

$$\tau_{run} \approx \frac{0.08}{\mathcal{M}_0^{2/3}(Nar_H)p^2}. \tag{44}$$

Evolutionary paths corresponding to the more realistic case of an "active" embryo depart from the runaway tracks when the embryo starts dominating disk dynamics in its vicinity, just as in

Figures 3-5. They smoothly switch to a behavior where $\mathcal{M}$ is a power law of time [similar behavior was obtained in Weidenschilling *et al.* (1997)]. Although this is consistent with the results of our qualitative analysis the exact value the power law index does not coincide with the value of 9/7 predicted by equation (34). In fact it is closer to 1 so that the embryo's mass grows linearly with time. We have found that the time dependence of mass can be roughly described by the following relation:

$$\mathcal{M}(\tau) \approx 1300\ (Nar_H)^{1.63} p^{1.4} \tau. \tag{45}$$

There is a simple explanation of this apparent discrepancy: when the embryo dominates the disk heating it induces strong nonuniformities in the distribution of the planetesimal surface density around it. As a result the instantaneous surface density of planetesimals at the embryo's location which determines its accretion rate decreases with time. We illustrate this point in Figure 13 where we plot the instantaneous surface density of planetesimals near the embryo N_{inst} normalized by its initial value as a function of time τ for $Nar_H = 10^3$, $p = 10^{-3}$ and several different values of initial mass $\mathcal{M}_0$. Values of N_{inst} are computed from spatial profiles of N and S using the corresponding conversion found in Paper II; in calculating N_{inst} we exclude the contribution of the horseshoe orbits because they cannot approach the embryo very closely and be accreted. One can see that N_{inst} begins to vary strongly only after the embryo starts dominating the disk dynamics (where the color of dots changes to red); in this regime N_{inst} can drop by a factor of 10 or more because of the spatial redistribution of planetesimals in the disk. This is equivalent to a decrease of Nar_H which would otherwise be constant. As a result, the accretion rate diminishes and embryo's mass grows slower than equation (34) would predict. The small variations of N_{inst} that occur in the stage when planetesimal dynamics is determined only by planetesimal scattering (blue dots) are explained by our exclusion of planetesimals on horseshoe orbits[8]: the spatial extent of the horseshoe region depends on the eccentricity and inclination of the planetesimals (see Paper III for details) which vary with time; this causes N_{inst} to change.

Our simple theory presented in §2.3 does not account for the local decrease of the planetesimal surface density as $\mathcal{M}$ the planetesimals are accreted onto the embryo. This is a considerable drawback which requires a more sophisticated treatment. We will not pursue this subject in this paper, merely note on its importance. Luckily it does not affect the general picture of the evolution of embryo-disk system described in §2.3, up to the isolation mass $\mathcal{M}_{is}$.

Note a very strong increase of the embryo's growth timescale in Figures 7-9 as one moves towards the outer edge of the nebula. The dimensionless timescale (in units of τ) grows because it strongly depends on parameter p characterizing embryo's accretion cross-section and p diminishes when the distance from the central star a increases. The timescale measured in physical units is additionally lengthened by the growth of the planetesimal synodic period t_{syn} with a: $t_{syn} \propto a^{3/2}$.

[8]In this regime the planetesimal disk is almost homogeneous; if we did not exclude planetesimals on the horseshoe orbits N_{inst} would be exactly constant.

As a result the most favorable conditions for the embryo's growth exist in the inner parts of the nebula. We will return to this issue in §4.

In Figures 10-12 we plot the dependence of s on time in the same way as we did it for $\mathcal{M}$. Initially (when planetesimal encounters control disk dynamics) one would expect s to behave in accordance with equation (30) which is exhibited by dotted line. Deviations from this power-law solution are caused by additional logarithmic dependence present in equation (30). At some point evolution switches to the embryo-dominated regime. We have used Figures 10-12 to determine the locations of the corresponding transition points for each track by approximately picking the point at which there is a break in the $s(\tau)$ dependence. As we have discussed above, this choice of the transition points agrees well with other characteristic indicators e.g. splitting of $\mathcal{M}(\tau)$ for "passive" and "active" embryo tracks in 7-9. When τ becomes very large system evolves in the asymptotic regime and s grows as a power-law of τ with index close to 5/9. This particular dependence and the fact that $\mathcal{M}(\tau) \propto \tau$ in the asymptotic regime conspire to produce the dependence of $\mathcal{M}(s)$ which is very close to that predicted analytically [see (28) and (42)]. The fact that the power-law index of $s(\tau)$ is different from 5/7 predicted by (34) is again explained by the drop of N_{inst} in the asymptotic regime: since embryo grows slower that expected it heats up planetesimal population nearby less efficiently than our analysis of §2.3 predicts. Nevertheless, by the end of our calculations planetesimal velocity dispersion in the heated zone exceeds the random velocity in the distant part of the nebula typically by a factor of several. As expected, the gravitational influence of the embryo considerably speeds up the dynamical evolution of the planetesimals in the heated zone. This behavior is in general agreement with the results of multi-zone simulations by Weidenschilling *et al.* (1997).

4. Discussion.

4.1. Results and their applications.

The most important result of our investigation is the elucidation of the role played by the coupling between the *nonuniform* disk dynamics and the embryo's mass growth. We have found in agreement with the previous investigations (Ida & Makino 1993; Tanaka & Ida 1997; Paper I) that the dynamical excitation of the planetesimal disk by the gravity of growing protoplanetary embryo dramatically changes the simple runaway picture of planetary growth, which is derived for homogeneous planetesimal disks. Using our results we can also study quantitatively the question of how long is required for the embryo to form?

As we have pointed out in §3, embryo accretes all the material within its feeding zone and reaches the isolation only after it settles into the asymptotic evolutionary regime (and not on the runaway stage). The time that the embryo spends on this asymptotic stage dominates the final timescale of its evolution. Indeed, for all the values of Nar_H and p explored in §3 the runaway timescale is usually shorter by a factor of several than the time needed for the embryo

to reach isolation in the asymptotic stage. This might indicate that the estimates of the embryo formation timescale produced by the conventional coagulation simulations neglecting the effects of inhomogeneous disk evolution could be off by a substantial factor.

For example, in the case $Nar_H = 400$, $p = 0.004$ typical for the planet formation in the terrestrial planet region of MMSN, the time needed for "passive" runaway embryo (thin solid curve) with $M_e/m = 10$ to reach the isolation mass $\approx 3 \times 10^{26}$ g is $\approx 4 \times 10^4$ yr; growth to the same mass for an "active" embryo that affects the disk would take $\approx 3 \times 10^5$ yr (see Figure 7) — almost a factor of 10 increase! This difference is even more striking for larger initial M_e/m for which runaway timescales are very short.

The very long time needed for the embryo's growth which arises in our calculations exacerbates the timescale problem for the growth of the rocky cores of the giant planets, because this process usually takes at least as long as the gaseous nebula is supposed to last: at 3.6 AU in the MMSN (a situation described by $p = 10^{-3}$ and $Nar_H = 10^3$ in our computations) the growth of M_e to 2×10^{27} g [the isolation mass given by (38)] takes 10^7 yr, while reaching 9×10^{27} g [isolation mass given by (39) which accounts for the expansion of the feeding zone due to the excitation of planetesimal random motions] would take 5×10^7 yr. Not only is this timescale is too long, it is also not clear that the isolation mass is large enough to trigger the core instability which would allow giant planets to accrete their huge gaseous mass (Mizuno 1980; Bodenheimer & Pollack 1986). Post-isolation chaotic dynamical evolution of the embryos (Chambers 2001) is the most likely solution of the latter problem, but it would require even more time for building up massive gas-accreting planetary cores. Note that the existence of this post-runaway chaotic evolutionary stage would not be a problem for the formation of terrestrial planets because (1) timescales are shorter in the inner parts of the nebula (see Figure 7), and (2) terrestrial planets did not accrete large amounts of gas which might indicate that they have formed after the gaseous nebula dispersed (which eliminates the time constraint related to the nebular dispersal).

It is true that in our calculations the isolation mass is usually larger than $\mathcal{M}_{is}$ reached by the embryos growing in the runaway regime in homogeneous disks: in the runaway stage $\mathcal{M}_{is}$ is given by (38) since it is typically reached in the shear-dominated regime (see Figures 3-5) while for the "active" embryos $\mathcal{M}_{is}$ is increased as a result of the strong excitation of planetesimal random velocities by the embryo, see equation (39). This simplifies the formation of massive rocky cores (at 3.6 AU $\mathcal{M}_{is}$ is increased by almost a factor of 5, see above). Unfortunately, the time required to reach larger $\mathcal{M}_{is}$ is longer as well.

The timescale issue becomes even more challenging for the growth of the outer giant planets if they formed at their present locations[9]: typical formation timescales are $\sim 10^9$ yr (see Figure 9) which is much longer than the timescale of the nebular dissipation (Hollenbach *et al.* 2000). One

[9]It was suggested by Thommes *et al.* (2002) that Uranus and Neptune were formed between the orbits of Jupiter and Saturn and were then scattered into their present orbits by these giant planets.

possibility to alleviate this problem would be to increase the surface density of planetesimals; this is a reasonable assumption beyond the so-called "snow line" (Hayashi 1981; Sasselov & Lecar 2002) where the condensation of ice takes place (at $1 - 3$ AU).

The fact that the embryo's growth does not stop when the embryo-planetesimal interaction starts to dominate disk dynamics and opens a gap is quite interesting. Previous estimates of the gap opening mass (Paper I; Ohtsuki & Tanaka 2002) only considered an embryo with a fixed mass and allowed plenty of time for the disk evolution. Under these conditions a gap would form in the planetesimal disk around the embryo when $T_{em} \approx T_{pl}$ and $\mathcal{M} \approx \mathcal{M}_{dd}(s)$; the instantaneous accretion rate of the embryo (if it were able to increase its mass) would be strongly affected even at this rather small value of $\mathcal{M}$. This would strongly slow down embryo's accretion at $\mathcal{M} \approx \mathcal{M}_{dd}(s)$. This reasoning essentially assumes that the disk instantaneously adjusts to any changes of the embryo's mass.

The picture turns out to be quite different in reality because the disk cannot quickly adapt to the embryo's evolution — on the contrary it is the embryo that initially evolves much faster than the disk when $\mathcal{M} > \mathcal{M}_{dd}$. As a result, during the time needed for the embryo's gravity to clear a gap in the disk its mass grows substantially. Although accretion in this part of s-$\mathcal{M}$ space is not in the runaway regime it is still quite fast initially; only after the embryo gains a considerable amount of mass the accretion smoothly changes its character to an orderly growth with $T_M \approx T_{em}$ in the region between the curves $\mathcal{M} = \mathcal{M}_{dd}$ and $\mathcal{M} = \mathcal{M}_{M-em}$. Thus, accretion sets into an orderly mode not when $T_{em} \approx T_{pl}$ (as analysis with a fixed embryo mass would assume) but only when $T_{em} \approx T_M$ which implies larger critical mass of the embryo[10].

Strong increase of the planetesimal velocity in the heated zone compared to that at infinity can be an important issue for the planetesimal growth in this region. Indeed, planetesimal coagulation in this part of the disk would almost certainly proceed in the orderly regime (in contrast to the embryo's accretion): planetesimal velocities should be so high that the gravitational focussing is negligible and accretion cross-section is independent of planetesimal velocities [see equation (3)]. Planetesimal agglomeration in the excited zone would then be so slow that the growth of more massive bodies in the heated region might essentially be chocked (planetesimal fragmentation would only strengthen this conclusion). New planetary embryos would be able to emerge only far enough from the preexisting ones where the planetesimal dynamics is not strongly affected by the gravitational perturbations of massive bodies.

It is also interesting to note that gravitational focussing is always important for the embryo's accretion (unlike the case of orderly growth, see §1). Focussing is weak when the planetesimal velocities are larger than the escape speed from the embryo's surface or when $S > p^{-1/2} \gg 1$ or $s > \mathcal{M}^{1/3} p^{-1/2}$ [see (A21)]. In Figures 3-5 we plot this restriction with a long-dash-dotted line ($S = p^{-1/2}$). One can see that evolutionary tracks never penetrate into this region: although

[10] As we have mentioned above this increase is not big enough to resolve the timescale issue.

initially S increases towards $p^{-1/2}$ as planetesimal velocity grows, the rapid increase of the embryo's mass caused by the runaway accretion makes S drop significantly (sometimes bringing embryo-planetesimal interaction into the shear-dominated regime) when the condition $T_M < T_{pl}$ is fulfilled, see §2.3 and equation (43). This implies that the embryo's accretion cross-section is *always* strongly increased over its geometric value by the gravitational focussing[11]. An important conclusion which can be drawn from this is that the growth of the embryo *never* proceeds in the orderly fashion with weak gravitational focussing, as proposed by Safronov (1972). Instead, it starts as a runaway evolution (Wetherill & Stewart 1989) which then switches to an oligarchic growth similar to that predicted by Kokubo & Ida (1998).

4.2. Limitations of the analysis.

The importance of our conclusions relies on the applicability of our simple model to the realistic protoplanetary disks. There is a lot of complications which can potentially affect our results. The assumption of a single mass population is certainly one of them. Our whole analysis relies on the possibility to compress the details of the planetesimal mass spectrum into properties of a single population with a unique characteristic mass. This is only possible if the estimates of such averaged mass characterizing separately the embryo's accretion and disk dynamical evolution agree with each other. If the distribution of masses and random velocities is such that this condition is not fulfilled (i.e. if embryo's accretion and disk dynamics are dominated by different parts of the planetesimal mass spectrum) then our consideration would fail and one would need to resort to a more intricate analysis.

Inclusion of a spectrum of planetesimal masses would also allow dynamical friction to redistribute the random energy of epicyclic motion between planetesimal populations with different masses (Stewart & Wetherill 1988). This might lead to an interesting situation when the embryo's interaction with different populations proceeds in different dynamical regimes — some will be in the shear-dominated regime while some in the dispersion-dominated. This can introduce some quantitative corrections to our results but we would expect the general picture of the planetary growth outlined here to remain unchanged: we have demonstrated in §2.3 that even with a single mass population of planetesimals we can still adequately reproduce the major features of the embryo's runaway growth.

Another potential worry is the *evolution* of the mass spectrum. This leads to the evolution of the average planetesimal mass m and affects Nar_H as a result. Note that changes of m can be caused not only by planetesimal coagulation which always tends to increase m but also by the change of the *shape* of the planetesimal mass spectrum driven by the embryo's presence. The last possibility might in principle lead to a *decrease* of m if the control over the embryo-disk evolution

[11]This also means that embryo's erosion by planetesimals colliding with it is unimportant.

switches to a lower-mass part of the planetesimal spectrum. Evolution of m is probably not very important initially because in the runaway regime the embryo grows faster than planetesimals, see equation (4). But later on when embryo dominates the disk dynamics and the system settles into the asymptotic regime with very slow accretion the planetesimal mass evolution might lead to some new effects. In addition, the growth of m is tightly coupled to the damping of the planetesimal epicyclic motion by inelastic scattering because both damping and coagulation are consequences of the same process — direct planetesimal collisions. Preliminary calculations demonstrate however that the decrease of planetesimal velocities by inelastic collisions would not allow embryo's accretion to continue in the runaway regime until the isolation mass is reached — at some point it would still switch to an orderly regime where $\mathcal{M}$ grows as some power law of time, although this orderly growth will be somewhat faster than that predicted by our analysis of §2.3 [see (34)]. Planetesimal fragmentation can also become important when relative planetesimal velocities exceed the escape speed from the planetesimal surface (roughly when $s \geq p^{-1/2}$). One can extend our analysis and numerical calculations to include at least the most important of these effects into account and we are going to do this in the future.

Our consideration has also been restricted to studying only a single embryo in the disk. In reality there would probably be many of them, at least initially. Since their masses grow by several orders of magnitude the Hill radii of neighboring embryos (as well as their excited regions) would overlap at some point. This would homogenize the disk to some extent but it would also slow down the accretion even more because disk would be heated by several embryos at a time. Finally gravitational perturbations between embryos would lead to their collisions and agglomeration. This question certainly deserves more attention both from the theoretical and from the numerical points of view. One should also be concerned with the possibility of embryo's migration which can in principle replenish the feeding zone of the embryo (Tanaka & Ida 1999; Ida *et al.* 2000).

Finally, gas drag can be important for the planetesimal dynamics especially for small planetesimal masses (Adachi *et al.* 1976). Its effect is similar to that of inelastic collisions — it damps epicyclic motions of planetesimals and leads to somewhat faster accretion by the embryo in the asymptotic regime. Gas drag can naturally be incorporated into our analytical apparatus of Paper II and its effects will be explored later on.

5. Conclusions.

In this paper we have self-consistently studied the dynamical evolution of a planetesimal disk coupled to the growth of a single massive protoplanetary embryo. We are able to demonstrate that the evolution of the embryo-disk system proceeds in two consecutive stages:

- It starts with a rapid runaway growth of the embryo, during which its mass is not large enough to affect the disk dynamics and the spatial distribution of planetesimals. On a rather short timescale (comparable to that arising in conventional coagulation simulations) the embryo

reaches the mass at which it takes over the control of the disk heating and runaway growth stops.

- After a short transient stage, the embryo-disk system settles into the asymptotic regime in which the timescale of the embryo's mass growth is comparable to the timescale on which the disk is heated by the embryo's gravity.

During the last stage, the embryo dynamically excites planetesimal epicyclic motions in its vicinity and repels the planetesimals forming a depression in the surface density of the guiding centers (see Figure 6). This effect produces a negative feedback for the embryo's accretion rate for two reasons: rapid growth of the random velocities of planetesimals leads to weaker gravitational focussing while the decrease of the instantaneous surface density (see Figure 13) reduces the amount of material available for accretion. As a result, growth of the protoplanetary embryo proceeds slower than in homogeneous planetesimal disks. This implies that conventional "particle-in-a-box" coagulation simulations (Wetherill & Stewart 1989; Kenyon & Luu 1998; Inaba *et al.* 2001) might be underestimating the timescale of the protoplanetary embryo's growth, sometimes by rather large factors (up to ~ 10). Multi-zone coagulation simulations (Spaute *et al.* 1991; Weidenschilling *et al.* 1997) should give a more reliable description of the protoplanetary disk evolution.

We have presented our equations in a dimensionless form which has allowed us to uncover a very important property of the problem we consider: its outcome depends on only two dimensionless parameters — the number of planetesimals inside the annulus of the disk with width equal to the planetesimal Hill radius r_H, Nar_H, and the ratio of the physical to Hill radii of a solid body (planetesimal or embryo) p. All astrophysically relevant characteristics of the system (m, a, M_c, Σ, ρ) are combined into these two parameters which greatly simplifies the exploration of the parameter space. We have numerically studied in §3 the evolution of the system for a number of pairs of Nar_H and p; combined with our analytical developments in §2 these results allow us to formulate a set of simple scaling relations (40)-(45) which can be used to predict the embryo-disk evolution for different sets of Nar_H and p.

To summarize we can say that the embryo's growth starts in the runaway regime, but then switches into the "oligarchic" growth of Kokubo & Ida (1998). We have demonstrated that the embryo's accretion never proceeds in the orderly regime with weak gravitational focussing suggested by Safronov (1972) — planetesimal velocities are always smaller than the escape velocity from the embryo's surface. The embryo formation timescale and some details of the embryo-disk evolution are subject to a number of uncertainties related to the simplicity of our model, as we discussed in §4. Nevertheless, we believe that our major conclusions are robust: the results of our qualitative analysis of §2 and numerical calculations presented in §3 suggest that the dynamical interaction between the protoplanetary embryo and planetesimal disk is a very important issue which should certainly be addressed when realistic coagulation simulations are performed. The general agreement between the results of our simple analysis of §2 with more accurate numerical calculations of §3 encourages the studies of more complex and more realistic problems in the same spirit. In the future

we are going to improve our treatment of the coupled planetesimal disk and embryo evolution by relaxing simplifying assumptions employed in this paper. We are also going to include additional mechanisms which are important in modelling of planetary formation — effects of multiple embryos, migration, gas drag, etc.

I am grateful to Scott Tremaine for his advice, and for reading this manuscript and making a lot of useful suggestions. The financial support of this work by the Charlotte Elizabeth Procter Fellowship and NASA grant NAG5-10456 is thankfully acknowledged.

REFERENCES

Adachi, I., Hayashi, C., & Nakazawa, K. 1976, Prog. Theor. Phys., 56, 1756

Bodenheimer, P. & Pollack, J. B. 1986, Icarus, 67, 391

Chambers, J. E. 2001, Icarus, 152, 205

Dones, L. & Tremaine, S. 1993, Icarus, 103, 67

Greenzweig, Y. & Lissauer, J. J. 1992, Icarus, 100, 440

Hasegawa, M. & Nakazawa, K. 1990, A&A, 227, 619

Hayashi, C. 1981, Progr. Theor. Phys. Suppl., 70, 35

Hollenbach, D. J., Yorke, H. W., & Johnstone, D. 2000, in *Protostars & Planets IV*, eds. Mannings, V., Boss, A. P., & Russell, S. S., 401

Ida, S. 1990, Icarus, 88, 129

Ida, S., Bryden, G., Lin, D. N. C., & Tanaka, H. 2000, ApJ, 534, 428

Ida, S., Kokubo, E., & Makino, J. 1993, MNRAS, 263, 875

Ida, S. & Makino, J. 1993, Icarus, 106, 210

Inaba, S., Tanaka, H., Nakazawa, K., Wetherill, G. W., & Kokubo, E. 2001, Icarus, 149, 235

Kokubo, E. & Ida, S. 1996, Icarus, 123, 180

Kokubo, E. & Ida, S. 1998, Icarus, 131, 171

Lissauer, J. J. 1987, Icarus, 69, 249

Malyshkin, L. & Goodman, J. 2001, Icarus, 150, 314

Mizuno, H. 1980, Progr. Theor. Phys., 96, 266

Ohtsuki, K. & Tanaka, H. 2002, submitted to Icarus

Petit, J.M. & Hénon, M. 1986, Icarus, 66, 536

Rafikov, R.R. 2001, AJ, 122, 2713, Paper I

Rafikov, R.R. 2002a, submitted to AJ, Paper II

Rafikov, R.R. 2002b, submitted to AJ, Paper III

Ruden S.P. 1999, in *The Origin of Stars and Planetary Systems*, eds. C. J. Lada & N. D. Kylafis; Kluwer Academic Publishers, 643

Safronov, V.S. 1972, *Evolution of the Protoplanetary Cloud and Formation of the Earth and Planets*, NASA TT-F-677

Safronov, V.S. 1991, Icarus, 94, 260

Sasselov, D.D. & Lecar, M. 2000, ApJ, 528, 995

Spaute, D., Weidenschilling, S. J., Davis, D. R., & Marzari, F. 1991, Icarus, 92, 147

Stevenson, D. J. 1982, Planet. Space Sci., 8, 755

Stewart, G. & Ida, S. 2000, Icarus, 143, 28

Stewart, G. & Wetherill, J. 1988, Icarus, 74, 542

Tanaka, H. & Ida, S. 1997, Icarus, 125, 302

Tanaka, H., & Ida, S. 1999, Icarus, 139, 350

Thommes, E. W., Duncan, M. J., & Levison, H. F. 2002, AJ, 123, 2862

Weidenschilling, S. J., Spaute, D., Davis, D. R., Marzari, F., & Ohtsuki, K. 1997, Icarus, 128, 429

Wetherill, G. W. & Stewart, G. R. 1989, Icarus, 77, 350

Wetherill, G. W. & Stewart, G. R. 1993, Icarus, 106, 190

AAS LaTeX macros v5.0.

A. More accurate equations of evolution.

Here we describe the system of equations we are going to use to follow the evolution of planetesimal surface density, eccentricity and inclinations. We derive these equations for the general case of a distribution of planetesimal masses for future applications. For this reason here N is a function of planetesimal mass[12] m.

We will use the following notation. First of all, we introduce the dimensionless radial distance from the embryo's orbit H, normalized by its Hill radius:

$$H = \Delta a / R_H, \quad R_H = a\mu_e^{1/3}, \quad \mu_e = M_e/M_c, \tag{A1}$$

where Δa is the dimensional radial distance from the embryo's orbit (equivalent to ha in the notation of Paper II). We also scale all eccentricities and inclinations by $R_H/a = \mu_e^{1/3}$. This gives us new variables S and S_z defined by equation (35). When doing this we have to keep in mind that S and S_z can vary not only because eccentricity and inclinations σ_e and σ_i vary with time but also because μ_e can change with time (as a consequence of planetary mass growth). This variation can be easily taken into account by noticing that

$$\frac{\partial}{\partial t}\left(N\{S,S_z\}^2\right) = \frac{1}{\mu_e^{2/3}}\frac{\partial}{\partial t}\left(N\sigma^2_{\{e,i\}}\right) - N\sigma^2_{\{e,i\}}\,\frac{2}{3}\frac{\partial \ln \mu_e}{\partial t}. \tag{A2}$$

We will characterize mass distribution of planetesimals by some fiducial mass $m_\star$ and introduce a dimensionless mass z such that

$$z = m/m_\star = \mu/\mu_\star, \quad \mu = m/M_c,\ \mu_\star = m_\star/M_c. \tag{A3}$$

Then $\mathcal{M} = M_e/m_\star$ Associated with this mass is a fiducial surface number density $N_\star = \Sigma_0/m_\star$, where Σ_0 is the total surface *mass* density of the disk. Following Papers II & III we assume both $N(m)$ and Σ_0 to be scaled by a^2 (so that $N(m) = N(z)$ is dimensionless, unlike §2). Finally we define a new surface number density function

$$g(z,H) = m_\star \frac{N(z)}{N_\star} = m_\star^2 \frac{N(z)}{\Sigma_0}, \qquad \int_0^\infty g(z,H) z dz = 1. \tag{A4}$$

We will use the notation $g_i(H)$ for the surface number density of planetesimals of mass m_i (or $z_i = m_i/m_\star$).

In transforming the planetesimal-planetesimal part of the evolution equations we will take into account that scattering coefficients in the dispersion-dominated regime have a rather specific form given by equations (82)-(93) of Paper II; we need to remember that expressions for these coefficients

[12] Unlike §2 where we have studied only a single mass population. We go back to this simpler case later on.

are functions of $\sigma_{e,i}$ normalized by Hill radius of planetesimal-planetesimal interaction r_H, which is different from S and S_z. With this in mind, using definitions (A1)-(A4) and equations (49)-(55) of Paper II and (13)-(15), (24)-(26), (B2) of Paper III we can finally represent equation of evolution of quantity $F = \{g, gs^2, gs_z^2\}$ in the following general form:

$$\frac{\partial F}{\partial \tau} = \pi N_\star \mu_\star^{1/3} \mathcal{M}^{-4/3} \frac{\partial F}{\partial \tau}\bigg|_{pl} + \mathcal{M}^{1/3} \left[\theta_1 \frac{\partial F}{\partial \tau}\bigg|_{hot} + \theta_2 \frac{\partial F}{\partial \tau}\bigg|_{cold} \right] - \frac{2}{3} F \frac{\partial \ln \mathcal{M}}{\partial \tau} \tag{A5}$$

with a new dimensionless time $\tau = (3/4\pi)\Omega t \mu_\star^{1/3} = t/t_{syn}$ [see (14)]. The interpolating functions $\theta_1 = \Theta(S, S_z)$ and $\theta_2 = 1 - \Theta(S, S_z)$ provide smooth matching between the shear- and dispersion-dominated regimes of embryo-planetesimal interaction (marked with subscripts "cold" and "hot", see Paper III). Function $\Theta(S, S_z)$ has the following properties: $\Theta(S, S_z) \to 1$ as $S, S_z \to \infty$, and $\Theta(S, S_z) \to 0$ as $S, S_z \to 0$. The last term in (A5) is present only in equations for eccentricity and inclination evolution.

For the surface density of planetesimals of type 1, $F = g_1$ and we have

$$\frac{\partial g_1}{\partial \tau}\bigg|_{pl} = -\frac{\partial}{\partial H}\left(\Upsilon_1^N g_1\right) + \frac{\partial^2}{\partial H^2}\left(\Upsilon_2^N g_1\right), \tag{A6}$$

$$\frac{\partial g_1}{\partial \tau}\bigg|_{hot} = -\frac{\partial}{\partial H}\left(|H|\langle \Delta\tilde{h}\rangle g_1\right) + \frac{\partial^2}{\partial H^2}\left(|H|\langle (\Delta\tilde{h})^2\rangle g_1\right), \tag{A7}$$

$$\frac{\partial g_1}{\partial \tau}\bigg|_{cold} = -g_1(H)|H| + \int\limits_{-\infty}^{\infty} \tilde{P}(H_0, H) g_1(H_0) |H_0| dH_0, \tag{A8}$$

where

$$\Upsilon_1^N(H) = 2 \int\limits_0^\infty dz_2 z_2 (z_1 + z_2) \int\limits_{-\infty}^{\infty} dH_1 |H_1| \langle \Delta\tilde{h}\rangle g_2(H - H_1), \tag{A9}$$

$$\Upsilon_2^N(H) = \int\limits_0^\infty dz_2 z_2^2 \int\limits_{-\infty}^{\infty} dH_1 |H_1| \langle (\Delta\tilde{h})^2\rangle g_2(H - H_1), \tag{A10}$$

where z_2 is used as a variable of integration over the planetesimal mass spectrum.

For eccentricity evolution, $F = 2g_1 S_1^2$ and

$$\frac{\partial}{\partial \tau}\left(2g_1 S_1^2\right)\bigg|_{pl} = \Upsilon_0^e g_1 - \frac{\partial}{\partial H}\left(\Upsilon_1^e g_1\right) + \frac{\partial^2}{\partial H^2}\left(\Upsilon_2^e g_1\right), \tag{A11}$$

$$\frac{\partial}{\partial \tau}\left(2g_1 S_1^2\right)\bigg|_{hot} = |H|\langle \Delta(\tilde{\mathbf{e}}^2)\rangle g_1 - \frac{\partial}{\partial H}\left(|H|\langle (\tilde{\mathbf{e}}^2 + 2\tilde{\mathbf{e}}\cdot\Delta\tilde{\mathbf{e}})\Delta\tilde{h}\rangle g_1\right)$$
$$+ \frac{\partial^2}{\partial H^2}\left(|H|\langle \tilde{\mathbf{e}}^2 (\Delta\tilde{h})^2\rangle g_1\right), \tag{A12}$$

$$\frac{\partial}{\partial \tau}\left(2g_1 S_1^2\right)\bigg|_{cold} = -2g_1(H) S_1^2(H)|H|$$

$$+\int\limits_{-\infty}^{\infty}\tilde{P}(H_0,H)g_1(H_0)\left(2s_1^2(H_0)+\frac{3}{4}\Delta(\tilde{\mathbf{e}}_{sc})^2(H_0)\right)|H_0|dH_0, \tag{A13}$$

where

$$\Upsilon_0^e(H)=2\int\limits_0^{\infty}dz_2z_2(z_1+z_2)\int\limits_{-\infty}^{\infty}dH_1|H_1|g_2(H-H_1)$$
$$\times\left[\frac{z_2}{z_1+z_2}\langle(\Delta\tilde{\mathbf{e}})^2\rangle+2\frac{S_1^2}{S_1^2+S_2^2}\langle\tilde{\mathbf{e}}\cdot\Delta\tilde{\mathbf{e}}\rangle\right], \tag{A14}$$
$$\Upsilon_1^e(H)=2\int\limits_0^{\infty}dz_2z_2(z_1+z_2)\int\limits_{-\infty}^{\infty}dH_1|H_1|g_2(H-H_1)$$
$$\times\left[2\frac{S_1^2S_2^2}{S_1^2+S_2^2}\langle\Delta\tilde{h}\rangle+\frac{S_1^4}{(S_1^2+S_2^2)^2}\langle\tilde{\mathbf{e}}^2\Delta\tilde{h}\rangle+2\frac{z_2}{z_1+z_2}\frac{S_1^2}{S_1^2+S_2^2}\langle(\tilde{\mathbf{e}}\cdot\Delta\tilde{\mathbf{e}})\Delta\tilde{h}\rangle\right], \tag{A15}$$
$$\Upsilon_2^e(H)=\int\limits_0^{\infty}dz_2z_2^2\int\limits_{-\infty}^{\infty}dH_1|H_1|g_2(H-H_1)$$
$$\times\left[2\frac{S_1^2S_2^2}{S_1^2+S_2^2}\langle(\Delta\tilde{h})^2\rangle+\frac{S_1^4}{(S_1^2+S_2^2)^2}\langle\tilde{\mathbf{e}}^2(\Delta\tilde{h})^2\rangle\right], \tag{A16}$$
$$S_1=S_1(H),\quad S_2=S_2(H-H_1). \tag{A17}$$

Different terms in the equation of evolution of $2g_1S_{z1}^2$ look analogous to (A11)-(A12) and (A14)-(A16) if we replace S with S_z but the shear-dominated part reads (see Paper III)

$$\frac{\partial}{\partial\tau}\left(2g_1S_{z1}^2\right)\Big|_{cold}=-2g_1(H)S_{z1}^2(H)|H|-2\int\limits_{-\infty}^{\infty}\tilde{P}(H_0,H)g_1(H_0)S_{z1}^2(H_0)|H_0|dH_0. \tag{A18}$$

In (A8), (A13), (A18) H_0 is an integration variable having the meaning of initial difference in semimajor axes of interacting bodies and

$$\tilde{P}(H_0,H)=\delta\left[H-H_0-\Delta\tilde{h}_{sc}(H_0)\right], \tag{A19}$$

where $\tilde{h}_{sc}(H_0)$ is some function for which the analytical prescription based on the results of numerical calculations exists (see Petit & Hénon 1987). Scattering coefficients $\langle\Delta\tilde{h}\rangle$, $\langle(\Delta\tilde{h})^2\rangle$, $\langle\tilde{\mathbf{e}}^2\Delta\tilde{h}\rangle$, $\langle(\tilde{\mathbf{e}}\cdot\Delta\tilde{\mathbf{e}})\Delta\tilde{h}\rangle$, $\langle\tilde{\mathbf{e}}^2(\Delta\tilde{h})^2\rangle$, $\langle(\Delta\tilde{\mathbf{e}})^2\rangle$, $\langle\tilde{\mathbf{e}}\cdot\Delta\tilde{\mathbf{e}}\rangle$ in these equations are functions of S,S_z, e.g.

$$\langle\Delta\tilde{h}\rangle=-\frac{4}{3}\frac{\ln\Lambda}{S_r^2S_{zr}^2}e^{-H^2/(2S_r^2)}\frac{1}{H}U_0^0\left(\frac{H/S_r}{2\sqrt{2}}\frac{H/S_{zr}}{2\sqrt{2}}\right),$$
$$\Lambda=\mathcal{M}^{1/3}\frac{S_{zr}}{z_1+z_2}(c_1S_r^2+c_2S_{zr}^2)\gg1,\qquad S_r=\sqrt{S_1^2+S_2^2},\ S_{zr}=\sqrt{S_{z1}^2+S_{z2}^2}, \tag{A20}$$

where c_1 and c_2 are some constants (their numerical values are fixed approximately in Paper III), and function U_ρ^η is defined by equation (95) of Paper II. Scattering coefficients describing embryo-planetesimal interaction are analogous to (A20) but have $\Lambda = (c_1 S_r^2 + c_2 S_{zr}^2) S_{zr}/(z_1 + z_2)$.

For the growth of the planetary embryo's mass we can write using equations (42)-(44) of Paper III:

$$\frac{\partial \mathcal{M}}{\partial \tau} = \frac{4}{3} p N_\star \mu_\star^{1/3} \mathcal{M}^{2/3} \int\limits_0^\infty z dz$$
$$\times \left[\frac{\pi_1}{8} \int\limits_{-\infty}^{\infty} g(z,H) \frac{|H|}{S^2 S_z^2} e^{-H^2/(2S^2)} \left(\frac{p}{4} H^2 U_+ + 2U_- \right) dH + \frac{5\pi_2}{S_z} g^{inst}(z) \right], \qquad \text{(A21)}$$

where functions $\pi_1 = \Pi(S, S_z)$ and $\pi_2 = 1 - \Pi(S, S_z)$ are used to interpolate between the shear- and dispersion-dominated regimes of embryo-planetesimal interaction. Function $\Pi(S, S_z)$ has properties analogous to the properties of $\Theta(S, S_z)$ (see Paper III). The quantity g^{inst} in the second term in brackets is the instantaneous surface density of planetesimals at the embryo's location, which can be calculated using the conversion between N and N^{inst} described in Paper III. The dimensionless parameter p was defined in (14). The first terms in the square bracket describe the mass accretion rate in the dispersion-dominated and shear-dominated regime, respectively.

When a single mass population of planetesimals is considered one should use the planetesimal mass m as a fiducial mass $m_\star$ and set $g(z, H) = \delta(z-1) f(H)$, where $f(H)$ is a function of distance H only. Then the integration over z_2 in (A9), (A10), (A14)-(A16) trivially goes away. In this work we have only considered a single mass population of planetesimals.

One can easily notice that in agreement with the results of §2 there are only two free parameters present in equations (A5)-(A21): p — ratio of physical radius to the Hill radius of any object, and $N_\star \mu_\star^{1/3}$ — measure of the disk surface number density equivalent to Nar_H of §2 (in §2 N is dimensional). When the distribution of planetesimal masses exists the shape of the mass spectrum is also a prescribed input function (which can vary in time as a result of coagulation). Equations (A5)-(A21) constitute a closed set of equations describing the behavior of the embryo-disk system. Their numerical solutions are presented in §3.